

BdryGP: a new Gaussian process model for incorporating boundary information

Liang Ding*, Simon Mak^{†1} and C. F. Jeff Wu^{‡2}

Hong Kong University of Science and Technology*, Duke University[†] and Georgia Institute of Technology[‡]

Abstract: Gaussian processes (GPs) are widely used as surrogate models for emulating computer code, which simulate complex physical phenomena. In many problems, additional boundary information (i.e., the behavior of the phenomena along input boundaries) is known beforehand, either from governing physics or scientific knowledge. While there has been recent work on incorporating boundary information within GPs, such models do not provide theoretical insights on improved convergence rates. To this end, we propose a new GP model, called BdryGP, for incorporating boundary information. We show that BdryGP not only has improved convergence rates over existing GP models (which do not incorporate boundaries), but is also more resistant to the “curse-of-dimensionality” in nonparametric regression. Our proofs make use of a novel connection between GP interpolation and finite-element modeling.

MSC 2010 subject classifications: Primary 62G08, 62M40.

Keywords and phrases: Gaussian Process, Kriging, Computer Experiment, Uncertainty Quantification, Finite-element Modeling, High-dimensional Inputs.

1. Introduction

With advances in mathematical modeling and computation, complex phenomena can now be simulated via computer code. This code numerically solves a system of governing equations which represents the underlying science of the problem. Due to the time-intensive nature of these numerical simulations (Yeh et al., 2018), Gaussian processes (GPs; Sacks et al., 1989) are often used as surrogate models to emulate the expensive computer code. Let $\mathbf{x} \in \mathcal{X} = [0, 1]^d$ be a vector of d code inputs, and let $f(\mathbf{x})$ be its corresponding code output. The idea is to adopt a GP prior for $f(\cdot)$, then use the posterior process given data to infer code output at an unobserved input. GP emulators are now widely used to study a broad range of scientific and engineering problems, such as rocket engines (Mak et al., 2018), universe expansions (Kaufman et al., 2011) and high energy physics (Goh et al., 2013).

In many applications, there is additional knowledge on the phenomenon than simply computer code output, and incorporating such knowledge can improve GP predictive performance. This “physics-integrated” GP modeling has garnered much attention in recent years (Wheeler et al., 2014; Golchi et al., 2015; Wang

¹Mak’s work is supported by U. S. Army Research Office grant W911NF-17-1-0007.

²Wu’s work is supported by NSF grant DMS 1914632.

and Berger, 2016). We consider here a specific type of information called *Dirichlet boundaries* (Bazilevs and Hughes, 2007), which specifies the values of f along certain input boundaries. Dirichlet boundaries are often available from governing physics or from simple physical considerations (Tan, 2018). One example is the simulation of viscous flows (White and Corfield, 2006), widely used in climatology and high energy physics. Such flows are dictated by the complex Navier-Stokes equations (Temam, 2001), and can be very time-consuming to simulate. At the limits of certain variables (e.g., zero viscosity or fluid incompressibility), the Navier-Stokes equations can be greatly simplified for efficient, even closed-form, solutions (Kiehn, 2001; Humphrey and Delange, 2016). Incorporating this boundary information within the GP can allow for improved predictive performance.

Despite its promise, the integration of GPs with boundary information is largely unexplored in the literature, with the only reference being a recent paper by Tan (2018). In this paper, a flexible *Boundary Modified Gaussian Process* (BMGP) is proposed, which can integrate a broad range of boundaries by modifying the mean and variance structure of a stationary GP. Due in part to its modeling flexibility, the BMGP model is quite complicated and difficult to analyze theoretically. This raises an important open question: to what extent does incorporating boundary information improve convergence rates for GPs?

To address this, we propose a new GP model, called BdryGP, which has provably improved error rates when incorporating boundary information. The key novelty is a new Boundary Constrained Matérn (BdryMatérn) covariance function, which incorporates boundary information of the form:

$$\mathcal{F}_j^{[0]} := \{f(\mathbf{x}) : x_j = 0\}, \quad \text{or} \quad \mathcal{F}_j^{[1]} := \{f(\mathbf{x}) : x_j = 1\}. \quad (1)$$

The BdryMatérn covariance inherits the same smoothness properties as the tensor Matérn kernel, while constraining GP sample paths to satisfy (1) almost surely. Assuming boundaries of the form (1) is known for each variable $j = 1, \dots, d$, we prove two main results for BdryGP. The first is a *deterministic* L^p convergence rate for a *fixed* function $f \in \mathcal{H}_{mix}^{1,c}(\mathcal{X})$:

$$\|f - \hat{f}_n^{\text{BM}}\|_{L^p} = \mathcal{O}(n^{-1}), \quad 1 \leq p < \infty. \quad (2)$$

Here, n is the sample size, \hat{f}_n^{BM} is the BdryGP predictor, and $\mathcal{H}_{mix}^{1,c}(\mathcal{X})$ is the Sobolev space with mixed first derivatives satisfying (1). The second is a *probabilistic* uniform bound for a *random* function $Z(\cdot)$ following a GP with sample paths in $\mathcal{H}_{mix}^{1,c}(\mathcal{X})$:

$$\sup_{\mathbf{x} \in [0,1]^d} |Z(\mathbf{x}) - \mathcal{I}_n^{\text{BM}} Z(\mathbf{x})| = \mathcal{O}_{\mathbb{P}}(n^{-1} [\log n]^{2d - \frac{3}{2}}), \quad (3)$$

where $\mathcal{I}_n^{\text{BM}}$ is the BdryGP interpolation operator satisfying $\mathcal{I}_n^{\text{BM}} f = \hat{f}_n^{\text{BM}}$. Both rates require a sparse grid design (Bungartz and Griebel, 2004). Compared to existing GP rates (which do not incorporate boundary information), our BdryGP rates decay much faster in sample size n . (A full comparison is given

in Section 5.3.) Furthermore, by incorporating boundaries, our rates are also more resistant to the well-known “curse-of-dimensionality” in nonparametric regression (Geenens, 2011). Our proof makes use of a novel connection between GP interpolation and finite-element modeling (FEM).

This paper is organized as follows. In Section 2, we present the new BdryGP model and derive the BdryMatérn kernel. In Section 3, we establish a novel connection between the BdryGP predictor and the FEM interpolator. In Section 4, we connect the function space for FEM with the native space for the BdryMatérn kernel. Using these results, we then derive in Section 5 the main convergence rates for BdryGP, and verify these rates in Section 6 via numerical simulations. Section 7 concludes the paper.

2. The BdryGP model

We first give a brief review of GP modeling, then present a model specification for BdryGP.

2.1. Gaussian process modeling

Let $\mathbf{x} \in \mathcal{X}$ be an input vector on domain $\mathcal{X} = [0, 1]^d$, with $f(\mathbf{x})$ denoting its corresponding computer code output. In Gaussian process emulation (Sacks et al., 1989; Santner, Williams and Notz, 2003), $f(\cdot)$ is assumed to be a realization of a Gaussian process with mean function $\mu : \mathcal{X} \rightarrow \mathbb{R}$, and covariance function $k : \mathcal{X} \times \mathcal{X} \rightarrow \mathbb{R}$. Further details on GP modeling can be found in Adler (1981).

Suppose the code is evaluated at n input points $\mathbf{X} = \{\mathbf{x}_1, \dots, \mathbf{x}_n\} \subset \mathcal{X}$, yielding observations $f(\mathbf{X}) = [f(\mathbf{x}_1), \dots, f(\mathbf{x}_n)]^\top$. Given data $f(\mathbf{X})$, one can show that the conditional process $f(\cdot)|f(\mathbf{X})$ is still a GP, with mean function:

$$\hat{f}_n(\mathbf{x}) = \mu(\mathbf{x}) + k(\mathbf{x}, \mathbf{X})k^{-1}(\mathbf{X}, \mathbf{X}) [f(\mathbf{X}) - \mu(\mathbf{X})], \quad (4)$$

and covariance function:

$$k_n(\mathbf{x}, \mathbf{y}) = k(\mathbf{x}, \mathbf{y}) - k(\mathbf{x}, \mathbf{X})k^{-1}(\mathbf{X}, \mathbf{X})k(\mathbf{X}, \mathbf{y}). \quad (5)$$

Here, $k(\mathbf{X}, \mathbf{x}) = [k(\mathbf{x}, \mathbf{x}_1), \dots, k(\mathbf{x}, \mathbf{x}_n)]^\top$ denotes the covariance vector between design \mathbf{X} and a new point \mathbf{x} , $k(\mathbf{x}, \mathbf{X}) = k(\mathbf{X}, \mathbf{x})^\top$, and $k(\mathbf{X}, \mathbf{X})$ is the covariance matrix $[k(\mathbf{x}_i, \mathbf{x}_j)]_{i=1}^n_{j=1}^n$ over design points. The posterior mean $\hat{f}_n(\cdot)$ is typically used as a predictor (or emulator) for unknown code output $f(\cdot)$, since it is optimal under quadratic and absolute error loss (Santner, Williams and Notz, 2003). The posterior variance $k_n(\mathbf{x}, \mathbf{x})$ then quantifies the uncertainty of the predictor $\hat{f}_n(\mathbf{x})$ at a new input setting \mathbf{x} .

The kernel k is also associated with an important function space $\mathcal{H}_k(\mathcal{X})$, called the *reproducing kernel Hilbert space* (RKHS) or *native space* of k Wendland (2010). For a symmetric, positive definite kernel k , the RKHS $\mathcal{H}_k(\mathcal{X})$ of k is

defined as the closure of the linear function space:

$$\left\{ \sum_{i=1}^n c_i k(\cdot, \mathbf{x}_i) : c_i \in \mathbb{R}, \mathbf{x}_i \in \mathcal{X}, n \in \mathbb{N} \right\}. \quad (6)$$

This RKHS is also endowed with an inner product $\langle \cdot, \cdot \rangle_k$ which satisfies the so-called *reproducing property*:

$$f(\mathbf{x}) = \langle f, k(\cdot, \mathbf{x}) \rangle_k, \quad \mathbf{x} \in \mathcal{X}, \quad (7)$$

for any function $f \in \mathcal{H}_k(\mathcal{X})$. Both the RKHS $\mathcal{H}_k(\mathcal{X})$ and its reproducing property will play a key role in the derivation and analysis of the BdryGP.

2.2. Boundary information

In many problems, boundary information on f is available from governing physical principles or scientific knowledge. We consider here a common type of boundary called Dirichlet boundaries (Bazilevs and Hughes, 2007), which specify the values of f along certain boundaries of the input domain $\mathcal{X} = [0, 1]^d$. In particular, we consider boundaries of the form $\mathcal{F}_j^{[0]}$ or $\mathcal{F}_j^{[1]}$ in (1), which quantify the values of f along the left hyperplane $\mathcal{S}_j^{[0]} := \{\mathbf{x} : x_j = 0\}$ or right hyperplane $\mathcal{S}_j^{[1]} := \{\mathbf{x} : x_j = 1\}$ of a variable x_j , respectively. We will call $\mathcal{F}_j^{[0]}$ and $\mathcal{F}_j^{[1]}$ the *left* and *right* boundary condition of variable x_j . Boundaries of this form arise naturally in many limiting simplifications of physical systems, and provide closed-form expressions for the BdryMatérn kernel.

To distinguish which boundaries are known beforehand, let $I^{[0]} \subseteq [d] = \{1, \dots, d\}$ denote the variables with known *left* boundary condition, and let $I^{[1]} \subseteq [d]$ denote the variables with known *right* boundary condition. With $I^{[0]} = \emptyset$ and $I^{[1]} = \emptyset$, this reduces to the standard setting with no boundary information; with $I^{[0]} = [d]$ and $I^{[1]} = [d]$, this implies knowledge of f along the full boundary of \mathcal{X} . Figure 1 illustrates this in two dimensions, with known boundaries of f in blue. The left plot shows the case of $I^{[0]} = I^{[1]} = \{1, 2\}$, with the value of f known on all boundaries of $[0, 1]^2$. The middle plot shows $I^{[0]} = \{1, 2\}$, $I^{[1]} = \emptyset$, with f known only on the left boundaries of each variable. The right plot shows $I^{[0]} = \{1, 2\}$, $I^{[1]} = \{1\}$, with f known on both boundaries of x_1 and on the left boundary of x_2 .

To integrate such boundary information, we need to specify two ingredients for BdryGP. First, a mean function $\mu(\cdot)$ is needed which satisfies known boundary conditions on f . Second, a covariance function $k(\cdot, \cdot)$ is needed which satisfies $k(\mathbf{x}, \mathbf{x}) = 0$ for any $\mathbf{x} \in \mathcal{S}_j^{[0]}$, $j \in I^{[0]}$ and any $\mathbf{x} \in \mathcal{S}_j^{[1]}$, $j \in I^{[1]}$. This ensures the BdryGP model satisfies the desired boundary information on f almost surely.

2.3. Mean function specification

Consider first the specification of the BdryGP mean function $\mu(\cdot)$. We adopt a simple strategy for constructing $\mu(\cdot)$ via an interpolator on known boundary

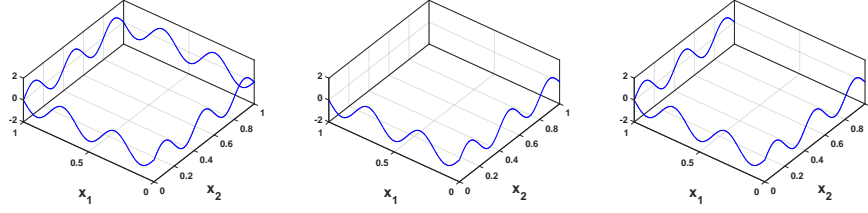


FIG 1. Visualizing $I^{[0]} = I^{[1]} = \{1, 2\}$ (full boundaries; left), $I^{[0]} = \{1, 2\}, I^{[1]} = \emptyset$ (left boundaries; middle), and $I^{[0]} = \{1, 2\}, I^{[1]} = \{1\}$ (right) for a 2-d function.

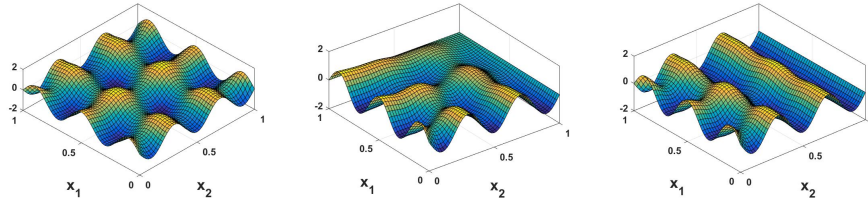


FIG 2. Proposed mean function $\mu(\cdot)$ in (9) for the three boundary cases in Figure 1.

conditions. For a point $\mathbf{x} \in \mathcal{X}$, let $\mathcal{P}_j^{[0]}\mathbf{x}$ and $\mathcal{P}_j^{[1]}\mathbf{x}$ denote the projection of \mathbf{x} onto the subspaces $\mathcal{S}_j^{[0]}$ and $\mathcal{S}_j^{[1]}$, respectively. These projected points can be written explicitly as:

$$\begin{aligned} [\mathcal{P}_j^{[0]}\mathbf{x}]_k &= \begin{cases} x_k, & \text{if } j \neq k \\ 0, & \text{if } j = k \end{cases} \quad \text{for } j \in I^{[0]}, \\ [\mathcal{P}_j^{[1]}\mathbf{x}]_k &= \begin{cases} x_k, & \text{if } j \neq k \\ 1, & \text{if } j = k \end{cases} \quad \text{for } j \in I^{[1]}. \end{aligned} \quad (8)$$

Furthermore, let $\mathbf{P}(\mathbf{x}) = \{\mathcal{P}_j^{[0]}\mathbf{x} : j \in I^{[0]}\} \cup \{\mathcal{P}_j^{[1]}\mathbf{x} : j \in I^{[1]}\}$ be the set of all such projected points of \mathbf{x} on known boundaries.

With this, the mean function $\mu(\cdot)$ can then be constructed as:

$$\mu(\mathbf{x}) = \phi(\mathbf{x}, \mathbf{P}(\mathbf{x}))[\phi(\mathbf{P}(\mathbf{x}), \mathbf{P}(\mathbf{x}))]^{-1}f(\mathbf{P}(\mathbf{x})). \quad (9)$$

where $\phi(\cdot, \cdot)$ is a compactly supported, positive definite, radial basis kernel (Wendland, 2010). Here, $\mu(\mathbf{x})$ can be interpreted as a GP interpolant at \mathbf{x} , using boundary information at projected points $\mathbf{P}(\mathbf{x})$ as data. By the interpolation property of GPs, the proposed mean function must therefore satisfy the desired boundary conditions:

$$\left\{ \mu(\mathbf{x}) : \mathbf{x} \in \mathcal{S}_j^{[0]} \right\} = \mathcal{F}_j^{[0]}, \quad \forall j \in I^{[0]}, \quad \left\{ \mu(\mathbf{x}) : \mathbf{x} \in \mathcal{S}_j^{[1]} \right\} = \mathcal{F}_j^{[1]}, \quad \forall j \in I^{[1]}. \quad (10)$$

We find the radial basis kernel $\phi(\mathbf{x}_1, \mathbf{x}_2) = \max\{(1 - \|\mathbf{x}_1 - \mathbf{x}_2\|)^\nu, 0\}$ (Wendland, 2010) to work well in practice.

Figure 2 illustrates the proposed mean function $\mu(\cdot)$ in (9) using the earlier two-dimensional example (with known boundaries marked in blue). From the left plot, which shows the mean function $\mu(\cdot)$ for the full boundary case of $I^{[0]} = I^{[1]} = \{1, 2\}$, we see that $\mu(\cdot)$ satisfies the desired boundary conditions from Figure 1. The same is true for the middle and right plots, which shows the proposed $\mu(\cdot)$ given partial boundary information.

2.4. Covariance function specification

Consider next the specification of the covariance function $k(\cdot, \cdot)$ for BdryGP. We present below a new BdryMatérn covariance function which incorporates boundary information of the form (1). We first discuss the properties of the BdryMatérn kernel for modeling, then provide an explicit derivation of this kernel.

2.4.1. The BdryMatérn kernel

For variable x_j , the one-dimensional (1-d) BdryMatérn kernel is defined as:

$$k_{\omega_j}^{\text{BM}}(x, y) = \begin{cases} \frac{\sinh[\omega_j(x \wedge y)] \sinh[\omega_j(1 - x \vee y)]}{\sinh(\omega_j)}, & j \in I^{[0]} \cap I^{[1]} \quad (\text{full}) \\ \sinh[\omega_j(x \wedge y)] \exp[\omega_j(-x \vee y)], & j \in I^{[0]} \cap \overline{I^{[1]}} \quad (\text{left}) \\ \exp[\omega_j(x \wedge y)] \sinh[\omega_j(1 - x \vee y)], & j \in \overline{I^{[0]}} \cap I^{[1]} \quad (\text{right}) \\ \exp(-\omega_j|x - y|), & j \in \overline{I^{[0]}} \cap \overline{I^{[1]}} \quad (\text{none}). \end{cases} \quad (11)$$

Here, $x \wedge y = \min(x, y)$ and $x \vee y = \max(x, y)$, and $\sinh(\cdot)$ and $\cosh(\cdot)$ are the hyperbolic sine and cosine functions. The first case corresponds to known boundaries for both the left and right endpoints of x_j (i.e., *full* boundary information). The second and third cases correspond to known boundaries for only the left and only the right endpoints of x_j , respectively (i.e., *partial* boundary information). The last case is for *no* boundary information on x_j ; this reduces to the Matérn-1/2 correlation function.

Using (11), we adopt the following product form for the BdryMatérn covariance over all d variables:

$$k_{\omega}^{\text{BM}}(\mathbf{x}, \mathbf{y}) = \sigma^2 \prod_{j=1}^d k_{\omega_j}^{\text{BM}}(x_j, y_j), \quad (12)$$

where σ^2 is a variance parameter. This product form of the BdryMatérn kernel $k_{\omega}^{\text{BM}}(\mathbf{x}, \mathbf{y})$ yields a very useful native space, which can be connected to FEM for proving improved GP convergence rates.

To see why the BdryMatérn kernel (12) can incorporate boundary information, consider a simple 1-d setting with $\sigma^2 = 1$ and $\omega = 1$. Figure 3 visualizes the

process variance $k_\omega^{\text{BM}}(x, x)$ as a function of \mathbf{x} over $[0, 1]$, for the first three cases in (11). The left plot shows $k_\omega^{\text{BM}}(x, x)$ for the full boundary case, where *both* left and right boundaries are known. Here, the process variance equals zero at the endpoints $x = 0$ and $x = 1$, meaning the BdryGP constrains sample paths to satisfy the left and right boundaries almost surely. The middle plot show $k_\omega^{\text{BM}}(x, x)$ when *only* the left boundary is known. Here, the process variance equals zero only when $x = 0$, meaning all BdryGP sample paths satisfy the left boundary almost surely. A similar interpretation holds for the right plot, where *only* the right boundary known.

The wavelength parameter w_j in the BdryMatérn kernel (12) plays a similar role as the scale parameter in the Matérn kernel: it controls the smoothness of sample paths from the BdryGP. To visualize this, Figure 4 plots the process covariance $k_\omega^{\text{BM}}(0.5, x)$ between a point $x \in [0, 1]$ and a fixed point at 0.5, for difference choices of wavelength ω . The left plot shows, as $\omega \rightarrow \infty$, this covariance converges to zero everywhere *except* at $x = 0.5$, which suggests that for larger wavelengths ω , the sample paths from BdryGP become more rugged. The right plot shows, as $\omega \rightarrow 0^+$, this covariance converges to zero everywhere, *including* at $x = 0.5$. This suggests that the process variance $k_\omega^{\text{BM}}(x, x)$ becomes smaller as $\omega \rightarrow 0^+$, which results in smoother sample paths.

The 1-d BdryMatérn kernel (11) also has an inherent connection to the covariance functions for the Brownian bridge and the Brownian motion. Suppose either the left or right boundary is known for variable x_j . Taking wavelength $\omega_j \rightarrow 0^+$ for the normalized BdryMatérn kernel, we get:

$$k_j^{\text{BR}}(x, y) = \lim_{\omega_j \rightarrow 0^+} \frac{k_{\omega_j}(x, y)}{\omega_j} = \begin{cases} (x \wedge y)(1 - x \vee y), & j \in I^{[0]} \cap I^{[1]} \quad (\text{full}) \\ x \wedge y, & j \in I^{[0]} \cap \overline{I^{[1]}} \quad (\text{left}) \\ 1 - x \vee y, & j \in \overline{I^{[0]}} \cap I^{[1]} \quad (\text{right}). \end{cases} \quad (13)$$

The first case is the covariance function of a Brownian bridge, and the second and third cases are variants of the covariance function for a Brownian motion. We will call $k_j^{\text{BR}}(x, y)$ the 1-d *Brownian kernel*, and its product form:

$$k^{\text{BR}}(\mathbf{x}, \mathbf{y}) = \prod_{j=1}^d k_j^{\text{BR}}(x_j, y_j) \quad (14)$$

the *Brownian kernel*. The link between the BdryMatérn kernel (used in BdryGP) and the Brownian kernel will serve as the basis for proving improved convergence rates via finite-element modeling. We note that the Brownian kernel is *not* used for modeling purposes, but rather as a theoretical tool for bridging the BdryGP model with FEM.

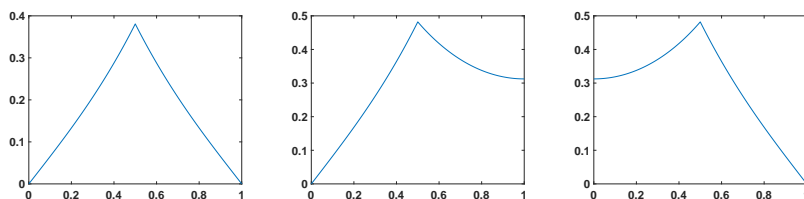


FIG 3. Visualizing the BdryGP variance $k_{\omega}^{\text{BM}}(x, x)$ over $x \in [0, 1]$ for full boundary (left), left boundary (middle), and right boundary (right) information.

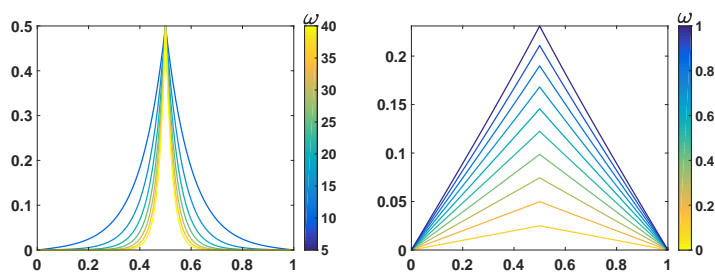


FIG 4. Visualizing the BdryGP covariance $k_{\omega}^{\text{BM}}(0.5, x)$ for full boundary information, with wavelength $\omega \rightarrow \infty$ (left) and $\omega \rightarrow 0^+$ (right).

2.4.2. Derivation under boundary conditions

We now provide a derivation of the 1-d BdryMatérn kernel (11). Consider the 1-d Matérn kernel:

$$k_{\nu, \omega}(x, y) = \frac{2^{1-\nu}}{\Gamma(\nu)} (\sqrt{2\nu\omega}|x-y|)^{\nu} K_{\nu}(\sqrt{2\nu\omega}|x-y|), \quad (15)$$

where ν is the smoothness parameter, ω is the scale parameter, and K_{ν} is the modified Bessel function (Abramowitz and Stegun, 1965). Let $S_{\nu, \omega}(s)$ denote the spectral density of $k_{\nu, \omega}$ (Cressie, 1991). With \simeq denoting equality up to an independent constant, the inner product of the RKHS $\mathcal{H}_{k_{\nu, \omega}}$ can be written as:

$$\langle f, g \rangle_{k_{\nu, \omega}} \simeq \int_{\mathbb{R}} \frac{\hat{f}(s)\hat{g}(s)}{S_{\nu, \omega}(s)} ds, \quad f, g \in \mathcal{H}_{k_{\nu, \omega}}, \quad (16)$$

where \hat{f} is the Fourier transform of f . Let $m = \nu + \frac{1}{2}$, and suppose $m \in \mathbb{N}$. Equation (16) then simplifies to:

$$\langle f, g \rangle_{k_{\nu, \omega}} \simeq \langle f, \mathcal{L}_{\nu, \omega} g \rangle_{L^2}, \quad (17)$$

where $D^l = d/dx^l$, $\mathcal{L}_{\nu,\omega}$ is the self-adjoint differential operator:

$$\mathcal{L}_{\nu,\omega} := \sum_{l=0}^m (-1)^l \binom{m}{l} C_{\nu,\omega}^{m-l} C'_{\nu,\omega}{}^l D^{2l}, \quad C_{\nu,\omega} = 2\nu\omega^2 C''_{\nu,\omega}, \quad C'_{\nu,\omega} = 4\pi^2 C''_{\nu,\omega}, \quad (18)$$

and $C''_{\nu,\omega} = \{2\pi^{1/2}\Gamma(\nu + 1/2)(2\nu)^\nu \omega^{2\nu} / \Gamma(\nu)\}^{-1/(\nu+1/2)}$.

With this, the reproducing property of the RKHS gives:

$$f(x) = \langle k_{\nu,\omega}(x, \cdot), f \rangle_{\mathcal{H}_{k_{\nu,\omega}}} = \int_{\mathbb{R}} k_{\nu,\omega}(x, y) \mathcal{L}_{\nu,\omega} f(y) dy, \quad \forall f \in \mathcal{H}_{k_{\nu,\omega}}. \quad (19)$$

This suggests that the Matérn kernel $k_{\nu,\omega}(x, y)$ is the Green's function of the differential operator $\mathcal{L}_{\nu,\omega}$, and can therefore be *uniquely* obtained by solving the following differential equation for k (Zaitsev and Polyanin, 2002):

$$\mathcal{L}_{\nu,\omega} k(x, y) = \delta(x - y), \quad (20)$$

where $\delta(x - y)$ is the Dirac delta function. This link serves as the basis for deriving the 1-d BdryMatérn kernel.

Consider next the case of full boundary information on f . This information can be incorporated into the Matérn RKHS $\mathcal{H}_{k_{\nu,\omega}}$ by restricting all functions $f \in \mathcal{H}_{k_{\nu,\omega}}$ to satisfy $f(0) = f(1) = 0$. The corresponding kernel k for this constrained function space must satisfy the reproducing property:

$$f(x) = \int_{\mathbb{R}} k(x, y) \mathcal{L}_{\nu,\omega} f(y) dy, \quad \forall f \in \mathcal{H}_{k_{\nu,\omega}}, \quad f(0) = f(1) = 0, \quad (21)$$

or equivalently, the following constrained differential equation:

$$\mathcal{L}_{\nu,\omega} k(x, y) = \delta(x - y), \quad k(0, y) = k(1, y) = 0. \quad (22)$$

For the cases of only left and only right boundary information, a similar reasoning gives the differential equations:

$$\mathcal{L}_{\nu,\omega} k(x, y) = \delta(x - y), \quad k(0, y) = 0, \quad \text{and} \quad (23)$$

$$\mathcal{L}_{\nu,\omega} k(x, y) = \delta(x - y), \quad k(1, y) = 0, \quad (24)$$

respectively.

The following proposition shows that the 1-d BdryMatérn kernel cases in (11) satisfy the above differential equations with $\nu = 1/2$, with their corresponding RKHS related to the weighted first-order Sobolev space:

$$\mathcal{H}_\omega^1 = \left\{ f : \omega \|f\|_{L^2}^2 + \frac{1}{\omega} \|Df\|_{L^2}^2 < \infty \right\}. \quad (25)$$

Proposition 1. *Suppose $\nu = 1/2$. The unique kernel k solving (22), (23) and (24) are the first three cases of the 1-d BdryMatérn kernel (11), with corresponding RKHS equal to \mathcal{H}_ω^1 with the additional constraint of $\{f(0) = 0, f(1) = 0\}$, $\{f(0) = 0\}$ and $\{f(1) = 0\}$, respectively.*

Proof. This can be proven by simply showing each of the first three cases of the 1-d BdryMatérn kernel (11) satisfies its corresponding differential equation (22), (23) or (24). Since a solution to these differential equations is unique, the uniqueness of the kernel then follows. The RKHS claim follows from the equivalence between the differential equations and its corresponding reproducing property. \square

This shows that the proposed BdryMatérn kernel indeed inherits the same smoothness properties as the Matérn-1/2 kernel, while also satisfying the desired boundary conditions.

Unfortunately, the same kernel derivation does not appear to extend for more general smoothness parameters $\nu > 1/2$, since more constraints are needed on kernel k in order to solve the corresponding differential equation. For example, when $\nu = 3/2$, a unique solution to (22) requires boundary conditions on both k and its first derivative, which implies further boundary information on f than the Dirchlet boundaries assumed in the paper.

3. Interpolation: BdryGP and FEM

With the BdryGP in hand, we now reveal a useful connection between FEM and the BdryGP predictor. This connection allows us to extend results from FEM to prove improved convergence rates for BdryGP.

3.1. Finite-Element Modeling

We begin with a brief review of FEM. Consider first the following partial differential equation (PDE) system:

$$\begin{cases} \mathcal{L}f(\mathbf{x}) = g(\mathbf{x}), & \mathbf{x} \in \mathcal{X}, \\ f(\mathbf{x}) = 0, & \mathbf{x} \in \partial\mathcal{X}. \end{cases} \quad (26)$$

Here, f is a solution on a Hilbert space \mathcal{V} , $\partial\mathcal{X}$ is the boundary of \mathcal{X} , and \mathcal{L} is a differential operator on \mathcal{V} . Under regularity conditions, the Lax-Milgram Theorem (Evans, 2015) ensures the existence of a unique weak solution satisfying (26).

The idea behind FEM is to approximate (26) on a discretization of \mathcal{X} . This requires two ingredients: a discretization mesh on \mathcal{X} , and a finite-dimensional function space constructed from this mesh. Given a multi-index $\boldsymbol{\alpha} = (\alpha_1, \dots, \alpha_d) \in \mathbb{N}^d$, let \mathcal{X} be discretized on the full grid mesh:

$$\mathbf{X}_{\boldsymbol{\alpha}} = \{ \mathbf{x}_{\boldsymbol{\alpha}, \boldsymbol{\beta}} = [\beta_j 2^{-\alpha_j}]_{j=1}^d : \beta_j \in \mathcal{B}_{\boldsymbol{\alpha}} \}, \quad (27)$$

where $\mathcal{B}_{\boldsymbol{\alpha}}$ is the index set:

$$\mathcal{B}_{\boldsymbol{\alpha}} = \{ \mathbf{1}_{\{j \in I^{[0]}\}}, \dots, 2^{\alpha_j} - \mathbf{1}_{\{j \in I^{[1]}\}} \}. \quad (28)$$

The mesh size of \mathbf{X}_α then becomes $h_\alpha = (h_{\alpha_1}, \dots, h_{\alpha_d}) = (2^{-\alpha_1}, \dots, 2^{-\alpha_d})$.

Next, given the mesh \mathbf{X}_α , let \mathcal{V}_α be the finite-dimensional function space spanned by first-order polynomials within each hypercube formed by \mathbf{X}_α (we discuss \mathcal{V}_α in greater detail in Section 4). The FEM solution is then defined as the projection of the weak solution f on the finite-dimensional space \mathcal{V}_α . Using a connection to Lagrange polynomial interpolation (see Chapter 15.2 of Wendland, 2010), this FEM solution can be equivalently represented as:

$$\mathcal{I}_\alpha f = \sum_{\mathbf{x}_{\alpha,\beta} \in \mathbf{X}_\alpha} f(\mathbf{x}_{\alpha,\beta}) \phi_{\alpha,\beta}(\mathbf{x}), \quad (29)$$

where:

$$\phi_{\alpha,\beta}(\mathbf{x}) = \prod_{j=1}^d \max \left\{ 1 - \frac{|x - x_{\alpha_j,\beta_j}|}{2^{-\alpha_j}}, 0 \right\} \quad (30)$$

are piecewise-linear basis functions over each cube.

3.2. FEM and the Brownian kernel

We now reveal a novel connection between the FEM interpolator (29) and the GP predictor under the Brownian kernel k^{BR} , first for full grid designs then for sparse grid designs.

3.2.1. Full Grids

We first make this connection for full grid designs:

Theorem 1. *Suppose $I^{[0]} \cup I^{[1]} = [d]$, and assume the full grid design \mathbf{X}_α with $n = |\mathbf{X}_\alpha|$ points. For any $f \in \mathcal{H}_{mix}^{1,c}$, the posterior predictor \hat{f}_n^{BR} of a GP with mean function $\mu(\cdot)$ in (9) and Brownian kernel k^{BR} is equivalent to the FEM solution $\mathcal{I}_\alpha f$, i.e.:*

$$\hat{f}_n^{\text{BR}}(\cdot) = \mu(\cdot) + k^{\text{BR}}(\cdot, \mathbf{X}_\alpha) [k^{\text{BR}}(\mathbf{X}_\alpha, \mathbf{X}_\alpha)]^{-1} [f(\mathbf{X}_\alpha) - \mu(\mathbf{X}_\alpha)] = \mathcal{I}_\alpha f(\cdot). \quad (31)$$

In other words, assuming $I^{[0]} \cup I^{[1]} = [d]$ (i.e., there exists left or right boundary information for each of the d variables), the predictor \hat{f}_n^{BR} for a GP with Brownian kernel k^{BR} is equivalent to the FEM solution $\mathcal{I}_\alpha f$, under the full grid design (or mesh) \mathbf{X}_α .

The key idea in proving Theorem 1 is to show that, under the Brownian kernel k^{BR} , the matrix inverse $[k^{\text{BR}}(\mathbf{X}, \mathbf{X})]^{-1}$ has an explicit closed-form expression. Under this expression, the desired equivalence can be shown via an inductive argument on dimension d . This result can be viewed as an extension of Proposition 2 in Ding and Zhang (2018).

Proof. Without loss of generality (WLOG), we assume the setting of only known left boundaries, i.e., $I^{[0]} = [d]$, $I^{[1]} = \emptyset$, since the setting of $I^{[0]} \cup I^{[1]} = [d]$

follows immediately. Furthermore, since the mean function $\mu(\cdot)$ in (9) satisfies the desired boundary conditions, we can simply show that the claim holds for a zero-mean GP with Brownian kernel k^{BR} , under a boundary condition of zero. Let $k(\mathbf{x}, \mathbf{y}) := k^{\text{BR}}(\mathbf{x}, \mathbf{y})$ and $k_j(x_j, y_j) := k_j^{\text{BR}}(x_j, y_j)$, $j = 1, \dots, p$. We first prove the theorem for the base cases of $d = 1$ and $d = 2$, then show the claim holds for $d > 2$ via induction.

Consider first the base case of $d = 1$. Under the assumption of known left boundaries, $\mathbf{X}_\alpha = \{x_i = i2^{-\alpha} : i = 1, \dots, 2^\alpha\}$ with $x_0 = 0$ and $n := |\mathbf{X}_\alpha|$. By Theorem 2 of Ding and Zhang (2018), $k^{-1}(\mathbf{X}_\alpha, \mathbf{X}_\alpha)$ is a symmetric tridiagonal matrix with entries

$$[k^{-1}(\mathbf{X}_\alpha, \mathbf{X}_\alpha)]_{i,i} = \begin{cases} \frac{x_{i+1} - x_{i-1}}{(x_i - x_{i-1})(x_{i+1} - x_i)}, & \text{if } i < n \\ \frac{1}{x_n - x_{n-1}}, & \text{if } i = n \end{cases},$$

$$[k^{-1}(\mathbf{X}_\alpha, \mathbf{X}_\alpha)]_{i-1,i} = [k^{-1}(\mathbf{X}_\alpha, \mathbf{X}_\alpha)]_{i,i-1} = -\frac{1}{x_i - x_{i-1}}$$

for $i = 1, 2, \dots, n$. Given any point $x \in [0, 1]$, assume $x_i < x < x_{i+1}$. By straightforward calculations, we have

$$\hat{f}_n^{\text{BR}}(x) = \frac{x_{i+1} - x}{x_{i+1} - x_i} f(x_i) + \frac{x - x_i}{x_{i+1} - x_i} f(x_{i+1}) = \sum_{x_{\alpha,\beta} \in \mathbf{X}_\alpha} f(x_{\alpha,\beta}) \phi_{\alpha,\beta}(x).$$

This proves the base case of $d = 1$.

For clarity in the later inductive step, we will also show the case of $d = 2$. Here, $\mathbf{X}_\alpha = \times_{j=1}^2 \mathbf{X}_{\alpha_j} = \times_{j=1}^2 \{x_{\alpha_j,1}, x_{\alpha_j,2}, \dots\}$, and $k(\mathbf{x}, \mathbf{y}) = k_1(x_1, y_1)k_2(x_2, y_2)$. Let \mathbf{x} be a point in \mathcal{X} , and let $K_{\mathbf{x}}$ be the hypercube in \mathbf{X}_α containing \mathbf{x} with vertices $\{\mathbf{x}_{\alpha,(i_1,i_2)} : i_j = \beta_j, \beta_j + 1, j = 1, 2\}$. The vector $k^{-1}(\mathbf{X}_\alpha, \mathbf{X}_\alpha)k(\mathbf{X}_\alpha, \mathbf{x})$ can be decomposed as:

$$\begin{aligned} & k^{-1}(\mathbf{X}_\alpha, \mathbf{X}_\alpha)k(\mathbf{X}_\alpha, \mathbf{x}) \\ &= \{k_1^{-1}(\mathbf{X}_{\alpha_1}, \mathbf{X}_{\alpha_1}) \otimes k_2^{-1}(\mathbf{X}_{\alpha_2}, \mathbf{X}_{\alpha_2})\} \text{vec}([k_1(x_1, x_{\alpha_1,\beta_1})k_2(x_2, x_{\alpha_2,\beta_2})]_{\beta_1,\beta_2}) \\ &= \text{vec}(k_2^{-1}(\mathbf{X}_{\alpha_2}, \mathbf{X}_{\alpha_2})[k_1(x_1, x_{\alpha_1,\beta_1})k_2(x_2, x_{\alpha_2,\beta_2})]_{\beta_1,\beta_2} k_1^{-1}(\mathbf{X}_{\alpha_1}, \mathbf{X}_{\alpha_1})) \end{aligned}$$

where $\text{vec}(\mathbf{M})$ denotes the vectorization of the matrix \mathbf{M} . Define

$$\Phi^{[2]}(\mathbf{x}) := k_2^{-1}(\mathbf{X}_{\alpha_2}, \mathbf{X}_{\alpha_2})[k_1(x_1, x_{\alpha_1,\beta_1})k_2(x_2, x_{\alpha_2,\beta_2})]_{\beta_1,\beta_2} k_1^{-1}(\mathbf{X}_{\alpha_1}, \mathbf{X}_{\alpha_1}).$$

By straightforward calculations similar to the 1-d case, it follows that $\Phi^{[2]}(\mathbf{x})$ has only the four non-zero entries:

$$\begin{aligned} \Phi_{\beta_1,\beta_2}^{[2]}(\mathbf{x}) &= \phi_{\alpha_1,\beta_1}(x_1)\phi_{\alpha_2,\beta_2}(x_2), & \Phi_{\beta_1+1,\beta_2}^{[2]}(\mathbf{x}) &= \phi_{\alpha_1,\beta_1+1}(x_1)\phi_{\alpha_2,\beta_2}(x_2), \\ \Phi_{\beta_1,\beta_2+1}^{[2]}(\mathbf{x}) &= \phi_{\alpha_1,\beta_1}(x_1)\phi_{\alpha_2,\beta_2+1}(x_2), & \Phi_{\beta_1+1,\beta_2+1}^{[2]}(\mathbf{x}) &= \phi_{\alpha_1,\beta_1+1}(x_1)\phi_{\alpha_2,\beta_2+1}(x_2), \end{aligned}$$

where $\phi_{\alpha,\beta}$ is the hat function defined previously. Thus, the predictor \hat{f}_n^{BR} can

be rewritten as:

$$\begin{aligned}\hat{f}_n^{\text{BR}}(\mathbf{x}) &= \text{vec}[\Phi^{[2]}(\mathbf{x})]^\top f(\mathbf{X}_\alpha) \\ &= \sum_{i_1=\beta_1}^{\beta_1+1} \sum_{i_2=\beta_2}^{\beta_2+1} \Phi_{i_1, i_2}^{[2]}(x) f(x_{\alpha_1, i_1}, x_{\alpha_2, i_2}) \\ &= \sum_{\mathbf{x}_\alpha, \beta \in \mathbf{X}_\alpha} f(\mathbf{x}_\alpha, \beta) \phi_{\alpha, \beta}(\mathbf{x}),\end{aligned}$$

which proves the theorem for $d = 2$.

Consider next the inductive step on d . Here, the full grid becomes $\mathbf{X}_\alpha = \times_{j=1}^d \mathbf{X}_{\alpha_j} = \times_{j=1}^d \{x_{\alpha_j, 1}, x_{\alpha_j, 2}, \dots\}$. Let $\mathbf{x} \in \mathcal{X}$ and let K_i be the hyper-cube in \mathbf{X}_α containing \mathbf{x} with vertices $\{\mathbf{x}_{\alpha, (i_1, \dots, i_d)} : i_j = \beta_j, \beta_j + 1, j = 1, \dots, d\}$ as before. Suppose the inductive hypothesis:

$$\begin{aligned}\hat{f}_n^{\text{BR}}(\mathbf{x}) &= k(\mathbf{x}, \mathbf{X}_\alpha) [k(\mathbf{X}_\alpha, \mathbf{X}_\alpha)]^{-1} f(\mathbf{X}_\alpha) \\ &= \text{vec}[\Phi^{[d]}(\mathbf{x})]^\top f(\mathbf{X}_\alpha) \\ &= \sum_{i_1=\beta_1}^{\beta_1+1} \sum_{i_2=\beta_2}^{\beta_2+1} \dots \sum_{i_d=\beta_d}^{\beta_d+1} \Phi_{i_1, \dots, i_d}^{[d]}(\mathbf{x}) f(x_{\alpha_1, i_1}, x_{\alpha_2, i_2}, \dots, x_{\alpha_d, i_d}),\end{aligned}$$

where:

$$\Phi_{i_1, \dots, i_d}^{[d]}(\mathbf{x}) = \prod_{j=1}^d \phi_{\alpha_j, i_j}(x_j).$$

From this hypothesis, we can see that there are at most 2^d non-zeros entries on $\Phi^{[d]}(\mathbf{x})$, namely, the entries $\Phi_{i_1, \dots, i_d}^{[d]}(\mathbf{x})$ with $i_j = \beta_j$ or $\beta_j + 1$. Since \hat{f}_n^{BR} is the Lagrange polynomial interpolation of f and is continuous, this assumption is equivalent to $\hat{f}_n^{\text{BR}} = \mathcal{I}_\alpha f$.

Under this inductive hypothesis, consider the case for dimension $d + 1$. Here, the full grid design becomes $\mathbf{X}_\alpha = \mathbf{X}_{\alpha_{1:d}} \times \mathbf{X}_{\alpha_{d+1}}$. Now let $\mathbf{x} \in \mathcal{X}$ and let K_i be a hyper-cube in \mathbf{X}_α containing \mathbf{x} with vertices $\{\mathbf{x}_{\alpha, (i_1, \dots, i_d)} : i_j = \beta_j, \beta_j + 1, j = 1, \dots, d + 1\}$. Let $k(\mathbf{x}, \mathbf{y}) = k(\mathbf{x}_{1:d}, \mathbf{y}_{1:d}) k_{d+1}(x_{d+1}, y_{d+1})$. Then the vector $k^{-1}(\mathbf{X}_\alpha, \mathbf{X}_\alpha) k(\mathbf{X}_\alpha, \mathbf{x})$ becomes:

$$\begin{aligned}& k^{-1}(\mathbf{X}_\alpha, \mathbf{X}_\alpha) k(\mathbf{X}_\alpha, \mathbf{x}) \\ &= \left\{ k^{-1}(\mathbf{X}_{\alpha_{1:d}}, \mathbf{X}_{\alpha_{1:d}}) \otimes k_{d+1}^{-1}(\mathbf{X}_{\alpha_{d+1}}, \mathbf{X}_{\alpha_{d+1}}) \right\} \\ & \quad \text{vec}([k(\mathbf{x}_{1:d}, \mathbf{x}_{\alpha_{1:d}, \beta_{1:d}}) k_{d+1}(x_{d+1}, x_{\alpha_{d+1}, \beta_{d+1}})]_{\beta_{1:d}, \beta_{d+1}}) \\ &= \text{vec} \left\{ k_{d+1}^{-1}(\mathbf{X}_{\alpha_{d+1}}, \mathbf{X}_{\alpha_{d+1}}) \right. \\ & \quad \left. [k(\mathbf{x}_{1:d}, \mathbf{x}_{\alpha_{1:d}, \beta_{1:d}}) k_{d+1}(x_{d+1}, x_{\alpha_{d+1}, \beta_{d+1}})]_{\beta_{1:d}, \beta_{d+1}} k^{-1}(\mathbf{X}_{\alpha_{1:d}}, \mathbf{X}_{\alpha_{1:d}}) \right\}.\end{aligned}$$

Similarly, define:

$$\begin{aligned}\Phi(\mathbf{x})^{[d+1]} &= k_{d+1}^{-1}(\mathbf{X}_{\alpha_{d+1}}, \mathbf{X}_{\alpha_{d+1}}) \\ & \quad [k(\mathbf{x}_{1:d}, \mathbf{x}_{\alpha_{1:d}, \beta_{1:d}}) k_{d+1}(x_{d+1}, x_{\alpha_{d+1}, \beta_{d+1}})]_{\beta_{1:d}, \beta_{d+1}} k^{-1}(\mathbf{X}_{\alpha_{1:d}}, \mathbf{X}_{\alpha_{1:d}}).\end{aligned}$$

From the inductive hypothesis, we know that

$$k^{-1}(\mathbf{X}_{\alpha_{1:d}}, \mathbf{X}_{\alpha_{1:d}})k(\mathbf{X}_{\alpha_{1:d}}, \mathbf{x}_{1:d}) = \text{vec} \left(\Phi^{[d]}(\mathbf{x}_{1:d}) \right)$$

which is the vectorization of the sparse matrix $\Phi^{[d]}(\mathbf{x}_{1:d})$, which has at most 2^d non-zero entries. Hence, $\Phi^{[d+1]}(\mathbf{x})$ can be decomposed as:

$$\Phi^{[d+1]}(\mathbf{x}) = k_{d+1}^{-1}(\mathbf{X}_{\alpha_{d+1}}, \mathbf{X}_{\alpha_{d+1}}) \left[\text{vec}(\Phi^{[d]}(\mathbf{x}_{1:d})) k_{d+1}(x_{d+1}, x_{\alpha_{d+1}, \beta_{d+1}}) \right]_{\beta_{d+1}}$$

So there are at most 2^{d+1} non-zeros entries on $\Phi^{[d+1]}(\mathbf{x})$, namely, the entries $\Phi_{i_1, \dots, i_{d+1}}(\mathbf{x})$ where $i_j = \beta_j$ or $\beta_j + 1$. Incorporating this, we then have:

$$\begin{aligned} \hat{f}_n^{\text{BR}}(x) &= \sum_{i_1=\beta_1}^{\beta_1+1} \sum_{i_2=\beta_2}^{\beta_2+1} \cdots \sum_{i_{d+1}=\beta_{d+1}}^{\beta_{d+1}+1} \Phi_{i_1, \dots, i_{d+1}}(\mathbf{x}) f(x_{\alpha_1, i_1}, x_{\alpha_2, i_2}, \dots, x_{\alpha_{d+1}, i_{d+1}}) \\ &= \sum_{\mathbf{x}_{\alpha}, \beta \in \mathbf{X}} \phi_{\alpha, \beta}(\mathbf{x}) f(\mathbf{x}_{\alpha, \beta}) = \mathcal{I}_{\alpha} f(\mathbf{x}), \end{aligned}$$

which completes the inductive step. \square

3.2.2. Sparse Grids

One disadvantage of full grid designs is the so-called *curse-of-dimensionality*: both the design size and its corresponding prediction error grow exponentially in dimension d . To this end, we extend next the earlier equivalence between FEM and the Brownian kernel for a broader class of designs called *sparse grids* (Bungartz and Griebel, 2004), which “sparsify” a full grid by retaining only certain subgrids of interest. These designs are used later to prove the improved convergence rates for BdryGP.

We first provide a brief review of sparse grid designs. A sparse grid of level k , denoted as \mathbf{X}_k^{SP} , is defined as follows:

$$\mathbf{X}_k^{\text{SP}} = \bigcup_{k \leq |\alpha| \leq k+d-1} \mathbf{X}_{\alpha}, \quad |\alpha| := \sum_{j=1}^d \alpha_j. \quad (32)$$

In words, the sparse grid \mathbf{X}_k^{SP} is the union of full grids \mathbf{X}_{α} whose multi-indices α sums between k and $k + d - 1$. Figure 5 shows sparse grids of levels 1 to 4 in two dimensions; we see that sparse grids provide a sizable reduction in design size compared to full grids. This reduction plays a key role in providing relief from dimensionality in many numerical approximation problems (Wendland, 2010; Dick, Kuo and Sloan, 2013).

The FEM solution $\mathcal{I}_{\alpha} f$ in (29), previously defined for the full grid \mathbf{X}_{α} , can be extended analogously for sparse grids. Similar to before, let $\mathcal{V}_k^{\text{SP}}$ be the sum of the finite-dimensional function spaces for each of the component full grids in the

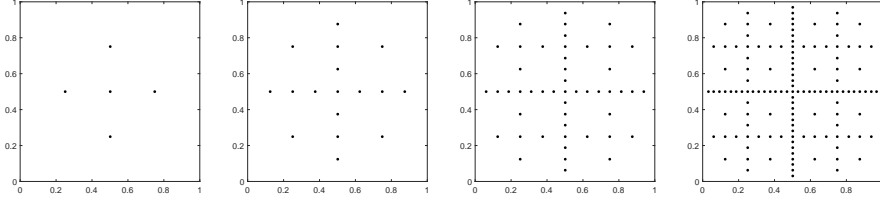


FIG 5. Sparse grid designs of levels 1 to 4 in two dimensions.

sparse grid (32). The FEM solution on sparse grid \mathbf{X}_k^{SP} , defined as the projection of the weak solution f on $\mathcal{V}_k^{\text{SP}}$, can be shown (Equation (28) of Garcke, 2012) to have the form:

$$\mathcal{I}_k^{\text{SP}} f = \sum_{j=0}^{d-1} (-1)^j \binom{d-1}{j} \sum_{|\alpha|=k+d-1-j} \mathcal{I}_\alpha f. \quad (33)$$

With this in hand, we show that under sparse grid designs, the FEM solution $\mathcal{I}_k^{\text{SP}} f$ is also equivalent to the GP posterior mean \hat{f}_n^{BR} with the Brownian kernel k^{BR} :

Theorem 2. *Suppose $I^{[0]} \cup I^{[1]} = [d]$, and assume the sparse grid design \mathbf{X}_k^{SP} with $n = |\mathbf{X}_\alpha|$ points. For any $f \in \mathcal{H}_{\text{mix}}^{1,c}$, the posterior predictor \hat{f}_n^{BR} of a GP with mean function (9) and Brownian kernel k^{BR} is equivalent to the FEM solution $\mathcal{I}_k^{\text{SP}} f$ in (33).*

Proof. In Theorem 1, we have shown the equivalence between the FEM solution $\mathcal{I}_\alpha f$ and the GP predictor \hat{f}_n^{BR} on the full grid design \mathbf{X}_α . Hence, $\mathcal{I}_\alpha f$ can be replaced by \hat{f}_n^{BR} in Equation (33). The result then follows by Algorithm 1 of Plumlee (2014). \square

3.3. FEM and the BdryMatérn kernel

Having proved the connection between FEM and the Brownian kernel k^{BR} , we then show how this relates to the BdryMatérn kernel k_ω^{BM} used in BdryGP. Of course, the GP predictors \hat{f}_n^{BR} and \hat{f}_n^{BM} under the Brownian and BdryMatérn kernels are not equivalent. However, we show below that the BdryGP approximation error $|f - \hat{f}_n^{\text{BM}}|$ can be upper bounded by the approximation error $|f - \hat{f}_n^{\text{BR}}|$ from the Brownian kernel:

Theorem 3. *Suppose $I^{[0]} \cup I^{[1]} = [d]$, and assume the sparse grid design \mathbf{X}_k^{SP} with $n = |\mathbf{X}_k^{\text{SP}}|$ points. Let \hat{f}_n^{BM} be the BdryGP predictor with mean function (9) and BdryMatérn kernel k_ω^{BM} . For any $f \in \mathcal{H}_{\text{mix}}^{1,c}$ and any $\omega > 0$:*

$$\|f - \hat{f}_n^{\text{BR}}\|_{L^\infty} \leq C \|f - \hat{f}_n^{\text{BM}}\|_{L^\infty}. \quad (34)$$

for some constant C independent of f , ω and n .

The proof of this theorem can be found in Appendix A.2.

4. Function spaces: BdryGP and FEM

Next, we prove the equivalence between the RKHS of the Brownian kernel k^{BR} , the constrained Sobolev space with mixed first derivatives, and the weak solution space for FEM.

4.1. Brownian Kernel RKHS and the Constrained Mixed Sobolev Space

We first establish the equivalence between the Brownian kernel RKHS and the mixed Sobolev space under boundary constraints. Let \mathcal{H}_{mix}^1 be the Sobolev space of functions with mixed first derivative:

$$\mathcal{H}_{mix}^1 := \{f : D^\alpha f \in L^2(\mathbb{R}^d), |\alpha|_\infty \leq 1\}. \quad (35)$$

where $|\alpha|_\infty = \max_{j \in [d]} |\alpha_j|$. Further let $\mathcal{H}_{mix}^{1,c}$ be the space of functions in \mathcal{H}_{mix}^1 with boundary value zero on known boundaries:

$$\mathcal{H}_{mix}^{1,c} := \left\{ f \in \mathcal{H}_{mix}^1 : f(\mathbf{x}) = 0 \text{ if } x_i \leq 0, i \in I^{[0]} \text{ or if } x_i \geq 1, i \in I^{[1]} \right\}. \quad (36)$$

We will call $\mathcal{H}_{mix}^{1,c}$ the *constrained* mixed Sobolev space.

The following proposition shows that the Brownian kernel RKHS $\mathcal{H}_{k^{\text{BR}}}$ and the constrained Sobolev space $\mathcal{H}_{mix}^{1,c}$ are equivalent function spaces:

Proposition 2. *The function spaces $\mathcal{H}_{k^{\text{BR}}}$ and $\mathcal{H}_{mix}^{1,c}$ are equivalent.*

Proof. By a straight-forward extension of Proposition 1, the Brownian kernel k^{BR} satisfies the following equation for any $f \in \mathcal{H}_{mix}^{1,c}$:

$$f(\mathbf{x}) = \int_{\mathbb{R}^d} D^1 f(\mathbf{s}) D^1 k^{\text{BR}}(\mathbf{x}, \mathbf{s}) d\mathbf{s} \quad (37)$$

From equation (37), the inner product of $\mathcal{H}_{k^{\text{BR}}}$ is:

$$\langle f, g \rangle_{\mathcal{H}_{k^{\text{BR}}}} = \int_{\mathbb{R}^d} D^\alpha f D^\alpha g d\mathbf{x}, \quad f, g \in \mathcal{H}_{mix}^{1,c}.$$

Thus, we only need to show the norm equivalence identity:

$$C_1 \|f\|_{\mathcal{H}_{k^{\text{BR}}}}^2 \leq \|f\|_{\mathcal{H}_{mix}^{1,c}}^2 \leq C_2 \|f\|_{\mathcal{H}_{k^{\text{BR}}}}^2.$$

Obviously, $C_1 = 1$. By the 1-d Poincaré inequality for locally absolutely continuous functions, there exists some constant C such that:

$$\int_{\mathbb{R}^d} [D^\alpha f]^2 \leq C \int_{\mathbb{R}^d} [D^1 f]^2, \quad \text{for any } |\alpha|_\infty \leq 1 \text{ and any } f \in \mathcal{H}_{mix}^{1,c}.$$

Iteratively applying the Poincaré inequality again, we get:

$$\|f\|_{\mathcal{H}_{mix}^{1,c}}^2 \leq 2^d C \|f\|_{\mathcal{H}_{k^{\text{BR}}}}^2$$

which proves the norm equivalence identity. \square

4.2. Hierarchical Difference Spaces

Next, we introduce the idea of a hierarchical difference space, which is widely used in FEM analysis. These spaces will allow for a multi-level decomposition of the finite-dimensional function spaces for FEM, and thereby the FEM solution as well.

Let us define the finite-dimensional function space \mathcal{V}_α for the FEM solution on full grid \mathbf{X}_α :

$$\mathcal{V}_\alpha := \text{span}\{\phi_{\alpha,\beta} : \mathbf{x}_{\alpha,\beta} \in \mathbf{X}_\alpha\} \quad (38)$$

where $\phi_{\alpha,\beta}$ is the earlier hat function with $\phi_{0,1}(x) = x$ and $\phi_{0,2}(x) = 1 - x$. It is clear that \mathcal{V}_α is the tensor product of these 1-d spaces, i.e., $\mathcal{V}_\alpha = \bigotimes_{j=1}^d \mathcal{V}_{\alpha_j}$.

Furthermore, \mathcal{V}_α can be represented as the following multi-level subspace decomposition:

$$\mathcal{V}_\alpha = \bigoplus_{\mathbf{0} \leq \alpha' \leq \alpha} W_{\alpha'}, \quad (39)$$

where $W_\alpha = \text{span}\{\phi_{\alpha,\beta} : \beta \in B_\alpha\}$ is called a *hierarchical difference space*. Further details on these spaces can be found in [Yserentant \(1986\)](#) and [Bungartz and Griebel \(2004\)](#). We note that, in order to incorporate partial boundaries, the hierarchical difference space used here is slightly modified from that in the literature. In the case of full boundaries (i.e., $I^{[0]} = I^{[1]} = [d]$), the two spaces are equivalent.

The subspace decomposition (39) allows for the following useful multi-level decomposition of the FEM solution. Consider first the FEM solution $\mathcal{I}_\alpha f$ on the full grid \mathbf{X}_α . From equation (39), $\mathcal{I}_\alpha f$ can be decomposed as:

$$\mathcal{I}_\alpha f = \sum_{\mathbf{0} \leq \alpha' \leq \alpha} f_{\alpha'}(\mathbf{x}). \quad (40)$$

Here, f_α is the projection of f on W_α , given by:

$$f_\alpha(\mathbf{x}) = \sum_{\beta \in B_\alpha} c_{\alpha,\beta} \phi_{\alpha,\beta}(\mathbf{x}), \quad (41)$$

and the constant $c_{\alpha,\beta}$ is known as the *hierarchical surplus*, defined as:

$$c_{\alpha,\beta} = \left(\prod_{j=1}^d A_{\alpha_j,\beta_j} \right) f(\mathbf{X}_\alpha), \quad A_{\alpha_j,\beta_j} = \begin{cases} [-\frac{1}{2} & 1 & -\frac{1}{2}] & \text{if } \alpha_j \geq 1 \\ [-1 & 1] & & \text{if } \alpha_j = 0 \end{cases}. \quad (42)$$

Here, $\prod_{j=1}^d A_{\alpha_j,\beta_j}$ denotes the Kronecker product of vectors A_{α_j,β_j} ; this is the standard stencil notation used in numerical analysis. Similarly, the sparse grid FEM solution $\mathcal{I}_k^{\text{SP}}$ can be decomposed as:

$$\mathcal{I}_k^{\text{SP}} f = \sum_{\mathbf{0} \leq |\alpha| \leq k+d-1} f_\alpha(\mathbf{x}). \quad (43)$$

This decomposition, along with the equivalences in Section 3, provides the basis for proving improved convergence rates for BdryGP.

4.3. Brownian Kernel RKHS and Hierarchical Difference Spaces

Consider now the limiting function space \mathcal{V} :

$$\mathcal{V} = \bigotimes_{j=1}^d \overline{\lim_{\alpha_j \rightarrow \infty} \mathcal{V}_{\alpha_j}}. \quad (44)$$

In other words, \mathcal{V} is the tensor product of the limiting 1-d finite-dimensional spaces in equation (38). The space \mathcal{V} can be viewed as the weak solution space on which FEM aims to solve the PDE system (26) in the limit.

The following proposition shows the equivalence of \mathcal{V} to the native space of k^{BR} :

Proposition 3. *The function spaces \mathcal{V} and $\mathcal{H}_{k^{\text{BR}}}$ are equivalent.*

The proof of this proposition requires the following lemma, which shows that the finite-dimensional RKHS of k^{BR} on grid \mathbf{X}_{α} is equivalent to \mathcal{V}_{α} .

Lemma 1. *The finite-dimensional spaces \mathcal{V}_{α} and $\{k^{\text{BR}}(\mathbf{x}_{\alpha,\beta}, \cdot) : \mathbf{x}_{\alpha,\beta} \in \mathbf{X}_{\alpha}\}$ are equivalent for any $\alpha \in \mathbb{N}^d$.*

The proof of Lemma 1 is given in Appendix A.1.

Proof (Proposition 3). From Lemma 1, we know that the projectors to \mathcal{V}_{α} and $\{k^{\text{BR}}(\mathbf{x}_{\alpha,\beta}, \cdot) : \mathbf{x}_{\alpha,\beta} \in \mathbf{X}_{\alpha}\}$ are equal for any $\alpha \in \mathbb{N}^d$. Since $\mathcal{H}_{k^{\text{BR}}}$ is the completion of the space $\lim_{\{\alpha_j \rightarrow \infty\}_{j=1}^d} \{k^{\text{BR}}(\mathbf{x}_{\alpha,\beta}, \cdot) : \mathbf{x}_{\alpha,\beta} \in \mathbf{X}_{\alpha}\}$, it is therefore the function space defined in equation (44). \square

Combining Propositions 2 and 3, we can then prove the desired equivalence between the two RKHSs $\mathcal{H}_{k^{\text{BR}}}$ and $\mathcal{H}_{k_{\omega}^{\text{BM}}}$, the constrained mixed Sobolev space $\mathcal{H}_{mix}^{1,c}$, and the weak solution space \mathcal{V} :

Theorem 4. *$\mathcal{H}_{k^{\text{BR}}}$, $\mathcal{H}_{k_{\omega}^{\text{BM}}}$, $\mathcal{H}_{mix}^{1,c}$ and \mathcal{V} are equivalent function spaces.*

Proof. Proposition 2 shows the equivalence between the RKHS $\mathcal{H}_{k^{\text{BR}}}$ and the constrained mixed Sobolev space $\mathcal{H}_{mix}^{1,c}$. Following the same reasoning (i.e., via the norm equivalence identity), the equivalence between the two RKHSs $\mathcal{H}_{k^{\text{BR}}}$ and $\mathcal{H}_{k_{\omega}^{\text{BM}}}$ can also be shown for any $\omega \in (0, \infty)$. The equivalence between $\mathcal{H}_{k^{\text{BR}}}$ and \mathcal{V} (Proposition 3) then completes the proof. \square

This function space equivalence allows for the decomposition of the RKHS $\mathcal{H}_{k^{\text{BR}}}$ (and its corresponding interpolator) into hierarchical difference subspaces (and its corresponding projections) of different levels. This decomposition plays a key role in proving the following convergence rates.

5. Convergence rates for BdryGP

With these equivalences in hand, we now prove the desired rates for BdryGP under sparse grids. All of these rates assume that $I^{[0]} \cup I^{[1]} = [d]$, i.e., at least one boundary is known for each of the d variables. Of course, the same rates also hold in the full boundary setting of $I^{[0]} = I^{[1]} = [d]$, where *all* boundaries of f are known.

5.1. L^p and L^∞ Convergence Rates

Suppose f is a *deterministic* function from the constrained mixed Sobolev space $\mathcal{H}_{mix}^{1,c}$. Under boundary information, the following theorem proves the L^p and L^∞ convergence rates for the proposed BdryGP (with BdryMatérn kernel k_ω^{BM}):

Theorem 5. *Suppose $I^{[0]} \cup I^{[1]} = [d]$, and assume the sparse grid design \mathbf{X}_k^{SP} with $n = |\mathbf{X}_k^{\text{SP}}|$ points. For any $f \in \mathcal{H}_{mix}^{1,c}$ and any wavelength ω , the BdryGP has an L^p convergence rate of:*

$$\|f - \hat{f}_n^{\text{BM}}\|_{L^p} = \mathcal{O}(n^{-1}), \quad 1 \leq p < \infty \quad (45)$$

and an L^∞ convergence rate of:

$$\|f - \hat{f}_n^{\text{BM}}\|_{L^\infty} = \mathcal{O}(n^{-1}[\log n]^{2(d-1)}). \quad (46)$$

The proof of Theorem 5 requires the following three lemmas. The first lemma (from [Bungartz and Griebel, 2004](#)) provides a big-O approximation of the number of points in the sparse grid \mathbf{X}_k^{SP} :

Lemma 2. *[Lemma 3.6 in [Bungartz and Griebel \(2004\)](#)] Let $n = |\mathbf{X}_k^{\text{SP}}|$ be the number of points in a d -dimensional sparse grid of level k . Then:*

$$n = \mathcal{O}(2^k[\log 2^k]^{d-1}).$$

The second lemma upper bounds the hierarchical surplus in $c_{\alpha,\beta}$ (42):

Lemma 3. *Let $f \in \mathcal{H}_{mix}^{1,c}$. Then there exists constants $C > 0$ and $\gamma \in (0, 1]$ independent of f , α and β , such that:*

$$|c_{\alpha,\beta}| \leq C2^{-(\gamma|\alpha|_\infty + |\alpha|)} \quad (47)$$

for almost all (α, β) , where $\alpha \in \mathbb{N}^d$ and $\beta \in B_\alpha$. Moreover, for any $\alpha \in \mathbb{N}^d$:

$$\sup_{\beta \in B_\alpha} |c_{\alpha,\beta}| \leq C2^{-|\alpha|}. \quad (48)$$

The last lemma provides a useful identity:

Lemma 4. *For any $x \in (0, 1)$,*

$$\sum_{i=0}^{\infty} x^i \binom{i+k+d-1}{d-1} = \sum_{j=0}^{d-1} \binom{k+d-1}{j} \left(\frac{x}{1-x}\right)^{d-1-j} \frac{1}{1-x}.$$

The proofs of Lemma 3 and 4 are found in the Appendix.

Proof. Consider first the prediction error $f - \hat{f}_n^{\text{BR}}$ for some $f \in \mathcal{H}_{mix}^{1,c}$, where \hat{f}_n^{BR} is the GP predictor using the Brownian kernel k^{BR} . Using (i) the function space equivalence $\mathcal{H}_{mix}^{1,c} = \mathcal{V}$ (Theorem 4) and (ii) the equivalence between \hat{f}_n^{BR} and the sparse grid FEM solution \hat{f}_n^{BR} (Theorem 2), this prediction error can be decomposed via (43):

$$f - \hat{f}_n^{\text{BR}} = f - \mathcal{I}_k^{\text{SP}} f = \sum_{\alpha \in \mathbb{Z}_{\geq 0}^d} f_\alpha - \sum_{0 \leq |\alpha| \leq k+d-1} f_\alpha = \sum_{|\alpha| \geq k+d} f_\alpha. \quad (49)$$

Therefore, the error can be bounded by the infinite series:

$$\|f - \hat{f}_n^{\text{BR}}\| \leq \sum_{|\alpha| \geq k+d} \|f_\alpha\| \quad (50)$$

for any norm $\|\cdot\|$.

Let us first take the L^p norm for $\|\cdot\|$ in (50). Note that

$$\begin{aligned} \|f - \hat{f}_n^{\text{BR}}\|_{L^p} &\leq \sum_{|\alpha| \geq k+d} \|f_\alpha\|_{L^p} \\ &= \sum_{|\alpha| \geq k+d} \left\| \sum_{\beta \in B_\alpha} c_{\alpha,\beta} \phi_{\alpha,\beta}(\mathbf{x}) \right\|_{L^p} \\ &= \sum_{|\alpha| \geq k+d} \left[\sum_{\beta \in B_\alpha} c_{\alpha,\beta}^p \int_{\mathbf{x}_{\alpha,\beta}-\mathbf{h}_\alpha}^{\mathbf{x}_{\alpha,\beta}+\mathbf{h}_\alpha} \phi_{\alpha,\beta}^p(\mathbf{x}) d\mathbf{x} \right]^{\frac{1}{p}} \\ &= \sum_{|\alpha| \geq k+d} \left[\frac{2^{d-1}}{(p+1)^d |B_\alpha|} \sum_{\beta \in B_\alpha} c_{\alpha,\beta}^p \right]^{\frac{1}{p}} \\ &\leq C \sum_{|\alpha| \geq k+d} 2^{-(\gamma|\alpha|_\infty + |\alpha|)} \\ &\leq C \sum_{|\alpha| \geq k+d} 2^{-(1+\varepsilon)|\alpha|}, \end{aligned} \quad (51)$$

where C and ε are positive constive constant independent of α (note that the constant C is used to show big-O convergence, and may change in value throughout the proof). Here, the third line follows from the fact that $\{\phi_{\alpha,\beta}\}_{\beta \in B_\alpha}$ is pairwise disjoint, the fourth line follows from the fact that $\int_{\mathbf{x}_{\alpha,\beta}-\mathbf{h}_\alpha}^{\mathbf{x}_{\alpha,\beta}+\mathbf{h}_\alpha} \phi_{\alpha,\beta}^p(\mathbf{x}) d\mathbf{x} = [2/(p+1)]^d 2^{-|\alpha|}$, and the fifth line follows from Lemma 3 (Equation 47).

We can further upper bound the last equation as follows:

$$\begin{aligned}
C \sum_{|\alpha| \geq k+d} 2^{-(1+\varepsilon)|\alpha|} &= C \sum_{i=k+d}^{\infty} 2^{-(1+\varepsilon)i} \sum_{|\alpha|=i} 1 \\
&= C \sum_{i=k+d}^{\infty} 2^{-(1+\varepsilon)i} \binom{i-1}{d-1} \\
&\leq C 2^{-(1+\varepsilon)k} \cdot 2^{-(1+\varepsilon)d} \sum_{i=0}^{\infty} 2^{-i} \binom{i+k+d-1}{d-1},
\end{aligned} \tag{52}$$

where the second line follows since there are $\binom{i-1}{d-1}$ ways to represent i as a sum of d natural numbers. With $x = 2^{-1}$, Lemma 4 gives:

$$\sum_{i=0}^{\infty} 2^{-i} \binom{i+k+d-1}{d-1} = 2 \sum_{j=0}^{d-1} \binom{k+d-1}{j} = 2 \frac{k^{d-1}}{(d-1)!} + \mathcal{O}(k^{d-2}). \tag{53}$$

Plugging (53) into (51), we get:

$$\begin{aligned}
\|f - \hat{f}_n^{\text{BR}}\|_{L^p} &\leq C \sum_{|\alpha| \geq k+d} 2^{-(1+\varepsilon)|\alpha|} \leq C 2^{-(1+\varepsilon)(k+d)} \frac{k^{d-1}}{(d-1)!} \\
&= C 2^{-(1+\varepsilon)k} \left[2^{-(1+\varepsilon)(d-1)} \frac{k^{d-1}}{(d-1)!} \right].
\end{aligned} \tag{54}$$

Using the upper bound on grid points for sparse grids (Lemma 2), the above prediction error can be stated in terms of sample size n :

$$\begin{aligned}
\|f - \hat{f}_n^{\text{BR}}\|_{L^p} &\leq C 2^{-\varepsilon k} 2^{-k} [\log 2^k]^{d-1} = 2^{-\varepsilon k} n^{-1} [k \log 2]^{2d-2} \\
&= \mathcal{O}(n^{-(1+\delta)}) = o(n^{-1})
\end{aligned}$$

for some $\delta > 0$.

For L^∞ convergence, we can take the L^∞ norm for $\|\cdot\|$ in (50) and mimic the same proof technique for L^p convergence, with the key distinction being the use of Lemma 3 (ii) in (51) to upper bound $\|\sum_{\beta \in B_\alpha} c_{\alpha,\beta} \phi_{\alpha,\beta}\|_{L^\infty} = \sup_{\beta \in B_\alpha} |c_{\alpha,\beta}| = \mathcal{O}(2^{-|\alpha|})$. This yields the following L^∞ rate in n :

$$\|f - \hat{f}_n^{\text{BR}}\|_{L^\infty} = \mathcal{O}(n^{-1} [\log n]^{2(d-1)}). \tag{55}$$

Finally, using Theorem 3, the L^p and L^∞ convergence rates for $\|f - \hat{f}_n^{\text{BR}}\|$ also hold for the BdryGP error $\|f - \hat{f}_n^{\text{BR}}\|$ as well, which completes the proof. \square

Remark 1: In Theorem 5, the intuition behind the slower L^∞ rate (compared to the L^p rate, $1 \leq p < \infty$), is that $D^1 f(\mathbf{x})$ can be ill-behaved on a measure-zero set on \mathcal{X} . Because of this, the pointwise convergence rate on this set can be much slower. The effect from this measure-zero set can be ignored under integration for \mathcal{L}^p with $p < \infty$.

Remark 2: We can further improve the convergence rate in Theorem 5 if we restrict f to the smaller function space $\mathcal{H}_{mix}^{2,c}$, the constrained Sobolev space with mixed *second* derivatives. Using the same proof strategy, but plugging in Lemma 3.5 in Bungartz and Griebel (2004), we can then show that $\|\hat{f}_n^{\text{BM}} - f\|_{L^2} = \mathcal{O}(n^{-2}[\log n]^{d-1})$ for $f \in \mathcal{H}_{mix}^{2,c}$. The function space equivalence (Theorem 4), however, does not hold under this extension, since $\mathcal{H}_{mix}^{2,c}$ is smaller than the RKHS of the BdryMatérn kernel $\mathcal{H}_{mix}^{1,c}$.

5.2. Probabilistic Uniform Rate

Next, we prove a probabilistic convergence rate for BdryGP, where f is assumed to be *random*, following a GP with sample paths in the constrained mixed Sobolev space $\mathcal{H}_{mix}^{1,c}$. This is motivated by the probabilistic convergence rates in Wang, Tuo and Wu (2018) for GPs without boundary constraints. Define first the following kernel space:

$$\mathcal{H}_{mix}^{1,c}(\mathcal{X} \times \mathcal{X}) := \{k(\mathbf{x}, \mathbf{y}) : k(\mathbf{x}, \cdot), k(\cdot, \mathbf{y}) \in \mathcal{H}_{mix}^{1,c}(\mathcal{X}), \forall \mathbf{x}, \mathbf{y} \in \mathcal{X}\}. \quad (56)$$

Such a space ensures that a GP with kernel $k \in \mathcal{H}_{mix}^{1,c}(\mathcal{X} \times \mathcal{X})$ has sample paths in $\mathcal{H}_{mix}^{1,c}$.

The following theorem gives a probabilistic uniform rate for BdryGP when f follows a GP with kernel $k \in \mathcal{H}_{mix}^{1,c}(\mathcal{X} \times \mathcal{X})$:

Theorem 6. *Suppose $I^{[0]} \cup I^{[1]} = [d]$, and assume the sparse grid design \mathbf{X}_k^{SP} with $n = |\mathbf{X}_k^{\text{SP}}|$. Let $Z(\cdot)$ be a GP with kernel $k \in \mathcal{H}_{mix}^{1,c}(\mathcal{X} \times \mathcal{X})$, and $\mathcal{I}_n^{\text{BM}}$ be the BdryGP interpolation operator satisfying $\mathcal{I}_n^{\text{BM}} f = \hat{f}_n^{\text{BM}}$. Then:*

$$\mathbb{E} \left[\sup_{\mathbf{x} \in \mathcal{X}} |Z(\mathbf{x}) - \mathcal{I}_n^{\text{BM}} Z(\mathbf{x})|^p \right]^{\frac{1}{p}} = \mathcal{O}(n^{-1}[\log n]^{2d-\frac{3}{2}}), \quad 1 \leq p < \infty, \quad (57)$$

and:

$$\sup_{\mathbf{x} \in \mathcal{X}} |Z(\mathbf{x}) - \mathcal{I}_n^{\text{BM}} Z(\mathbf{x})| = \mathcal{O}_{\mathbb{P}}(n^{-1}[\log n]^{2d-\frac{3}{2}}). \quad (58)$$

Proof. Let $Z(\cdot)$ be a GP with kernel $k \in \mathcal{H}_{mix}^{1,c}(\mathcal{X} \times \mathcal{X})$, and let $\mathcal{I}_n^{\text{BM}}|_{\mathbf{x}}$ and $\mathcal{I}_n^{\text{BM}}|_{\mathbf{y}}$ be the projection operator $\mathcal{I}_n^{\text{BM}}$ in arguments \mathbf{x} and \mathbf{y} . Consider the following hierarchical expansion of the so-called ‘‘natural distance’’ σ :

$$\begin{aligned} \sigma^2(\mathbf{x}, \mathbf{y}) &:= \mathbb{E}[(Z(\mathbf{x}) - \mathcal{I}_n^{\text{BM}} Z(\mathbf{x}))(Z(\mathbf{y}) - \mathcal{I}_n^{\text{BM}} Z(\mathbf{y}))] \\ &= k(\mathbf{x}, \mathbf{y}) - \mathcal{I}_n^{\text{BM}}|_{\mathbf{y}} k(\mathbf{x}, \mathbf{y}) - \mathcal{I}_n^{\text{BM}}|_{\mathbf{x}} k(\mathbf{x}, \mathbf{y}) - \mathcal{I}_n^{\text{BM}}|_{\mathbf{x}} \mathcal{I}_n^{\text{BM}}|_{\mathbf{y}} k(\mathbf{x}, \mathbf{y}) \\ &= \{I - \mathcal{I}_n^{\text{BM}}|_{\mathbf{x}}\} \{I - \mathcal{I}_n^{\text{BM}}|_{\mathbf{y}}\} k(\mathbf{x}, \mathbf{y}). \end{aligned}$$

By Theorem 5, we have:

$$\sigma(\mathbf{x}, \mathbf{y}) = \mathcal{O}(n^{-1}[\log n]^{2(d-1)})$$

for any $\mathbf{x}, \mathbf{y} \in \mathcal{X}$. This can then be plugged into the proof of Theorem 1 of in Wang, Tuo and Wu (2018) to prove the result. \square

TABLE 1
 Convergence rates for BdryGP and existing rates in the literature. “Optimal design” refers to optimally-chosen points under a statistical criterion or error bound.

Work	Design	Type	Rate
Current	Sparse grid	Deterministic, L^p	$\mathcal{O}(n^{-1})$
Current	Sparse grid	Deterministic, uniform	$\mathcal{O}(n^{-1}[\log n]^{2(d-1)})$
van de Geer (2000)	Optimal design	Deterministic, L^2	$\mathcal{O}(n^{-\frac{1}{2+d}})$
Wu and Schaback (1993)	Optimal design	Deterministic, uniform	$\mathcal{O}(n^{-\frac{1}{2d}})$
Current	Sparse grid	Probabilistic, uniform	$\mathcal{O}_{\mathbb{P}}(n^{-1}[\log n]^{2d-\frac{3}{2}})$
Wang, Tuo and Wu (2018)	Optimal Design	Probabilistic, uniform	$\mathcal{O}_{\mathbb{P}}(n^{-\frac{1}{2d}}[\log n^{\frac{1}{2d}}]^{\frac{1}{2}})$
Stein (1999)	Full grid	Mean square, pointwise	$\mathcal{O}(n^{-\frac{1}{2d}})$
Ritter (2000)	Optimal design	Mean square, L^2	$\mathcal{O}(n^{-\frac{1}{2d}})$

5.3. Comparison with Existing Results

We now compare these BdryGP rates to existing GP rates which do not incorporate boundary information. Table 1 summarizes several key results for the latter. Consider first the *deterministic* rates, where f is a deterministic function within a function space. For $f \in \mathcal{H}^1(\mathcal{X})$ (the first-order Sobolev space), Wu and Schaback (1993) proved a L^∞ minimax rate of $\mathcal{O}(n^{1/(2d)})$ for radial basis interpolators. Under the same assumptions, van de Geer (2000) and Gu (2002) also proved a L^2 minimax rate of $\mathcal{O}(n^{-1/(2+d)})$ for kernel ridge regression. Without additional information on f , these rates are in general not improvable (Stone, 1982). To contrast, by incorporating boundary information, the proposed BdryGP enjoys quicker convergence rates in sample size n , with an L^p rate of $\mathcal{O}(n^{-1})$ and an L^∞ rate of $\mathcal{O}(n^{-1}[\log n]^{2(d-1)})$. Furthermore, the BdryGP rates are more resistant to the “curse-of-dimensionality”. As dimension d grows large, the existing error rate $\mathcal{O}(n^{1/(2d)})$ grows exponentially in sample size n , whereas the BdryGP rates grow exponentially in a lower-order term $\log n$ (for L^∞) or in constants (for L^p). This shows that, by incorporating boundary information, the BdryGP not only yields lower prediction errors for fixed dimension d , but maintains relatively good performance as dimension d grows large.

Consider next the *probabilistic* uniform rates, where f follows a GP with kernel $k \in \mathcal{H}_{mix}^{1,c}(\mathcal{X} \times \mathcal{X})$, which ensures sample paths are contained in the constrained mixed Sobolev space $\mathcal{H}_{mix}^{1,c}$. These probabilistic uniform GP rates were first studied in Tuo, Wang and Wu (2017) for the Matérn kernel without boundary information. There, the authors proved an L^p rate over the stochastic process (uniform in x) of $\mathcal{O}(n^{-1/(2d)}\sqrt{[\log n^{1/(2d)}]})$, and a probabilistic rate (uniform in x) of $\mathcal{O}_{\mathbb{P}}(n^{-1/(2d)}\sqrt{[\log n^{1/(2d)}]})$. To contrast, by incorporating boundary information, the same uniform rates are improved to $\mathcal{O}(n^{-1}[\log n]^{2d-3/2})$ and $\mathcal{O}_{\mathbb{P}}(n^{-1}[\log n]^{2d-3/2})$ in Theorem 6, respectively. This again shows that, by incorporating boundary information, the BdryGP can yield lower prediction errors.

It is worth mentioning that the constrained *mixed* Sobolev space used here imposes greater smoothness than the Sobolev spaces used in existing rates, which

may also contribute to our rate improvements. To parse out the effect from different function spaces, we can directly extend results from [Rieger and Wendland \(2017\)](#) and [Tuo, Wang and Wu \(2017\)](#) to show that, under *unconstrained* function spaces of comparable smoothness to Theorems 5 and 6, we achieve only L^p rates of $\mathcal{O}(n^{-1/2}[\log n]^{(5/2)(d-1)})$ and $\mathcal{O}_{\mathbb{P}}(n^{-1/2}[\log n]^{(5/2)d-2})$ (a full proof is provided in the Appendix). These rates are of an order slower than the BdryGP rates in Theorems 5 and 6, which confirms that boundary information indeed improves predictive performance.

6. Numerical Experiment

We now provide a small simulation study verifying the improved error convergence rate of the proposed BdryGP model over standard GP models (which do not incorporate boundary information). The set-up is as follows. We use three $d = 10$ -dimensional test functions from the emulation literature, taken from [Surjanovic and Bingham \(2016\)](#):

$$\text{Corner peak: } f(\mathbf{x}) = \left(1 + \frac{\sum_{j=1}^d x_j}{d}\right)^{-d-1},$$

$$\text{Product peak: } f(\mathbf{x}) = \prod_{j=1}^d (1 + 10(x_j - 0.25)^2)^{-1},$$

$$\text{Rosenbrock: } f(\mathbf{x}) = 4 \sum_{j=1}^{d-1} (x_j - 1)^2 + 400 \sum_{j=1}^{d-1} ((x_j - 0.5) - 2(x_{j+1} - 0.5))^2.$$

We will compare two variants of the BdryGP model: (i) the BdryGP with *full* boundary information (i.e., $I^{[0]} = I^{[1]} = [d]$), and (ii) the BdryGP with only *partial* information on left boundaries (i.e., $I^{[0]} = [d]$, $I^{[1]} = \emptyset$), with a standard GP model with the product Matérn-1/2 kernel. All models use a wavelength parameter of $\omega = 1.0$, and are compared on the prediction error $\|f - \hat{f}\|_{L^1}$, which is approximated using 1000 uniformly sampled points in \mathcal{X} .

Figure 6 (top) plots the log-error $\|f - \hat{f}\|_{L^1}$ as a function of sample size n (and sparse grid level k). For all three functions, these log-errors appear to be linearly decreasing in sparse grid level k . Furthermore, the two BdryGP models (both of which incorporate some form of boundary information) yield much lower errors than the standard GP without boundary information, with the error decay slopes for BdryGP roughly double that for the standard GP model. This is in line with the convergence rates proven in Section 5, which show that the L^1 error rates for BdryGP are on the order of $\mathcal{O}(2^{-k})$, but increase to $\mathcal{O}(2^{-k/2})$ without boundary information.

To highlight the error gap between full and partial boundary information, Figure 6 (bottom) plots the L^1 error ratio of the full boundary BdryGP over the partial boundary BdryGP. All ratios are above 1.0, which shows that full boundaries indeed yield more information on f compared to partial boundaries.

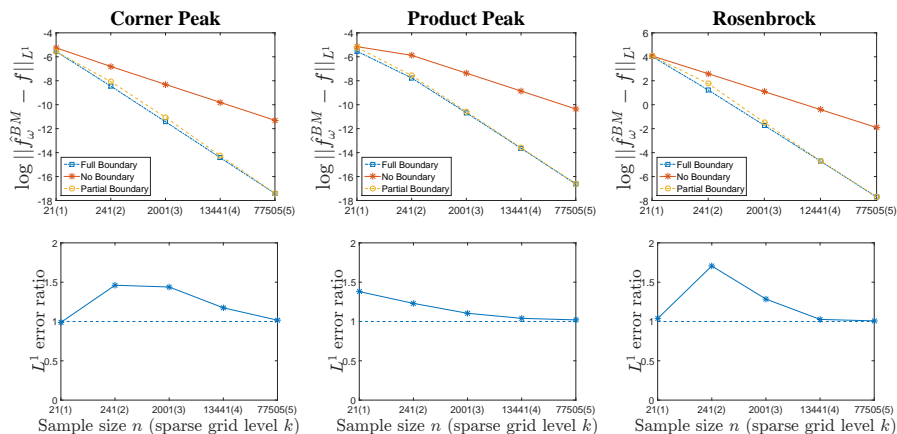


FIG 6. (Top): Log-error $\log \|\hat{f}_n^{BM} - f\|_{L^1}$ as a function of sample size n (and sparse grid level k). (Bottom): The L^1 error ratio of the full boundary GP over the partial boundary GP, as a function of sample size n (and sparse grid level k).

However, this improvement seems to diminish as sample size n grows large; this suggests that the information on f from design points can outweigh the additional information from full boundaries (over partial boundaries) for large sample sizes.

7. Conclusion

This paper presents a new Gaussian process model, called BdryGP, for incorporating one type of boundary information with provably improved convergence rates. The key novelty in BdryGP is a new BdryMatérn covariance function, which inherits the same smoothness properties of a tensor Matérn kernel, while constraining sample paths to satisfy boundary information almost surely. Using a new connection between finite-element modeling and GP interpolation, we then show that under sparse grid designs, BdryGP enjoys improved convergence rates over standard GP models, which do not account for boundary information. By incorporating boundaries, our BdryGP rates are also more resistant to the well-known “curse-of-dimensionality” in nonparametric regression. Numerical simulations confirm these improved convergence rates, and demonstrate the improved performance of BdryGP over standard GP models.

While this paper provides an appealing theoretical framework for the BdryGP model, there are further developments which would be useful for practical implementation. For computational efficiency, one can leverage the equivalence between FEM and BdryGP (Section 3) to eliminate matrix computation steps for prediction and likelihood evaluations, which improves the scalability of BdryGP for big datasets. It would also be useful to investigate the behavior of BdryGP (e.g., consistency and convergence rates) under maximum likelihood estimation of model parameters.

References

- ABRAMOWITZ, M. and STEGUN, I. A. (1965). *Handbook of Mathematical Functions: with Formulas, Graphs, and Mathematical Tables*. Courier Corporation.
- ADLER, R. J. (1981). *The Geometry of Random Fields*. Wiley.
- BARTHELMANN, V., NOVAK, E. and RITTER, K. (2000). High dimensional polynomial interpolation on sparse grids. *Advances in Computational Mathematics* **12** 273–288.
- BAZILEVS, Y. and HUGHES, T. J. (2007). Weak imposition of Dirichlet boundary conditions in fluid mechanics. *Computers & Fluids* **36** 12–26.
- BUNGARTZ, H.-J. and GRIEBEL, M. (2004). Sparse Grids. *Acta Numerica* **13** 1–123.
- CRESSIE, N. (1991). *Statistics for Spatial Data*, 2 ed. Wiley-Interscience.
- DICK, J., KUO, F. Y. and SLOAN, I. H. (2013). High-dimensional integration: The quasi-Monte Carlo way. *Acta Numerica* **22** 133–288.
- DING, L. and ZHANG, X. (2018). Scalable Stochastic Kriging with Markovian Covariances. *arXiv preprint*. <https://arxiv.org/abs/1803.02575>.
- EVANS, L. C. (2015). *Partial Differential Equations*, 2nd ed. AMS.
- GARCKE, J. (2012). *Sparse Grids in a Nutshell*. Springer.
- GEENENS, G. (2011). Curse of dimensionality and related issues in nonparametric functional regression. *Statistics Surveys* **5** 30–43.
- GOH, J., BINGHAM, D., HOLLOWAY, J. P., GROSSKOPF, M. J., KURANZ, C. C. and RUTTER, E. (2013). Prediction and computer model calibration using outputs from multifidelity simulators. *Technometrics* **55** 501–512.
- GOLCHI, S., BINGHAM, D. R., CHIPMAN, H. and CAMPBELL, D. A. (2015). Monotone emulation of computer experiments. *SIAM/ASA Journal on Uncertainty Quantification* **3** 370–392.
- GU, C. (2002). *Smoothing Spline ANOVA Models*. Springer.
- HUMPHREY, J. and DELANGE, S. L. (2016). *Introduction to Biomechanics*. Springer.
- KAUFMAN, C. G., BINGHAM, D., HABIB, S., HEITMANN, K. and FRIEMAN, J. A. (2011). Efficient emulators of computer experiments using compactly supported correlation functions, with an application to cosmology. *The Annals of Applied Statistics* **5** 2470–2492.
- KIEHN, R. (2001). Some closed form solutions to the Navier Stokes equations. *arXiv preprint*. <https://arxiv.org/abs/physics/0102002>.
- MAK, S., SUNG, C. L., YEH, S. T., WANG, X., CHANG, Y. H., JOSEPH, V. R., YANG, Y. and WU, C. F. J. (2018). An efficient surrogate model for emulation and physics extraction of large eddy simulations. *Journal of American Statistical Association* **113** 1443–1456.
- PLUMLEE, M. (2014). Fast prediction of deterministic functions using sparse grid experimental designs. *Journal of the American Statistical Association* **109** 1581–1591.
- RIEGER, C. and WENDLAND, H. (2017). Sampling inequalities for sparse grids. *Numerische Mathematik* **136** 439–466.
- RITTER, K. (2000). *Average-Case Analysis of Numerical Problems*. Springer.

- SACKS, J., WELCH, W. J., MITCHELL, T. J. and WYNN, H. P. (1989). Design and analysis of computer experiments. *Statistical Science* **4** 409-423.
- SANTNER, T. J., WILLIAMS, B. J. and NOTZ, W. I. (2003). *The Design and Analysis of Computer Experiments*. Springer.
- STEIN, M. L. (1999). Uniform asymptotic optimality of linear predictions of a random field using an incorrect second-order structure. *The Annals of Statistics* **18** 850-872.
- STONE, C. J. (1982). Optimal Global Rates of Convergence for Nonparametric Regression. *Annals of Statistics* **8** 1348-1360.
- SURJANOVIC, S. and BINGHAM, D. (2016). Virtual Library of Simulation Experiments: Test Functions and Datasets. <https://www.sfu.ca/~ssurjano/index.html>.
- TAN, M. H. Y. (2018). Gaussian process modeling with boundary information. *Statistica Sinica* **28** 621-648.
- TEMAM, R. (2001). *Navier-Stokes Equations: Theory and Numerical Analysis* **343**. American Mathematical Society.
- TUO, R., WANG, Y. and WU, C. F. J. (2017). Improved rates of convergence for kernel ridge regression, with application to Gaussian process models. Under review for *Annals of Statistics*. <https://docs.google.com/viewer?a=v&pid=sites&srcid=ZGVmYXVsdGRvbWFpbmxydWl0dW8yMDE3fGd4OjEzYzJkODU0YTc4YTg0ZDU>.
- VAN DE GEER, S. A. (2000). *Empirical Processes in M-estimation*. Cambridge University Press.
- WANG, X. and BERGER, J. O. (2016). Estimating shape constrained functions using Gaussian processes. *SIAM/ASA Journal on Uncertainty Quantification* **4** 1-25.
- WANG, W., TUO, R. and WU, C. F. J. (2018). On prediction properties of kriging: uniform error bounds and robustness. *Journal of the American Statistical Association*, to appear. <https://arxiv.org/abs/1710.06959>.
- WENDLAND, H. (2010). *Scattered Data Approximation*, 2nd ed. Cambridge University Press.
- WHEELER, M. W., DUNSON, D. B., PANDALAI, S. P., BAKER, B. A. and HERRING, A. H. (2014). Mechanistic hierarchical Gaussian processes. *Journal of the American Statistical Association* **109** 894-904.
- WHITE, F. M. and CORFIELD, I. (2006). *Viscous Fluid Flow*. McGraw-Hill New York.
- WU, Z. and SCHABACK, R. (1993). Local error estimates for radial basis function interpolation of scattered data. *IMA Journal of Numerical Analysis* **13** 13-27.
- YEH, S.-T., WANG, X., SUNG, C.-L., MAK, S., CHANG, Y.-H., ZHANG, L., WU, C. J. and YANG, V. (2018). Common proper orthogonal decomposition-based spatiotemporal emulator for design exploration. *AIAA Journal* **56** 2429-2442.
- YSERENTANT, H. (1986). On the multi-level splitting of finite element spaces. *Numerische Mathematik* **49** 379-412.
- ZAITSEV, V. F. and POLYANIN, A. D. (2002). *Handbook of Exact Solutions for Ordinary Differential Equations*, 2 ed. CRC Press.

Appendix A

A.1. Proof for Lemma 1

Proof. WLOG, we assume $I^{[0]} = [d]$ and $I^{[1]} = \emptyset$. Let

$$\bigotimes_{j=1}^d \Delta_j f(\mathbf{x}_{\alpha, \beta}) := \left(\prod_{j=1}^d A_{\alpha_j, \beta_j} \right) f(\mathbf{X})$$

denote the Hierarchical Surplus $c_{\alpha, \beta}$ where the operator Δ_i is defined as:

$$\Delta_i f(\mathbf{x}_{\alpha, \beta}) := \begin{cases} -\frac{1}{2}f(\mathbf{x}_{\alpha, \beta} + 2^{-\alpha_i} e_i) + f(\mathbf{x}_{\alpha, \beta}) - \frac{1}{2}f(\mathbf{x}_{\alpha, \beta} - 2^{-\alpha_i} e_i) & \text{if } \alpha_i \geq 1, \\ f(1) - f(0) & \text{if } \alpha_i = 0. \end{cases}$$

Obviously, Δ_i is a linear operator. Let $\pi_{\mathcal{V}_{\alpha}}[\cdot]$ be the projector to the space \mathcal{V}_{α} as the one in equation (3.19) in [Bungartz and Griebel \(2004\)](#). The projection operator $\pi_{\mathcal{V}_n}[\cdot]$ can be written as:

$$\begin{aligned} & \pi_{\mathcal{V}_n}[\cdot] \\ &= \sum_{|\alpha|_{\infty} \leq n} \sum_{\beta \in B_{\alpha}} \phi_{\alpha, \beta} \bigotimes_{i=1}^d \Delta_i \\ &= \sum_{|\alpha|_{\infty} \leq n} \sum_{\beta_d \in B_{\alpha}} \phi_{\alpha_d, \beta_d} \Delta_d \sum_{\beta_{d-1} \in B_{\alpha}} \phi_{\alpha_{d-1}, \beta_{d-1}} \Delta_{d-1} \cdots \sum_{\beta_1 \in B_{\alpha}} \phi_{\alpha_1, \beta_1} \Delta_1 \\ &= \sum_{\alpha_d \leq n_d} \sum_{\beta_d \in B_{\alpha}} \phi_{\alpha_d, \beta_d} \Delta_d \sum_{\alpha_{d-1} \leq n_{d-1}} \sum_{\beta_{d-1} \in B_{\alpha}} \phi_{\alpha_{d-1}, \beta_{d-1}} \Delta_{d-1} \cdots \sum_{\alpha_1 \leq n_1} \sum_{\beta_1 \in B_{\alpha}} \phi_{\alpha_1, \beta_1} \Delta_1. \end{aligned}$$

As a result the posterior mean of BdryGP with Brownian kernel $\hat{f}_{\mathbf{n}}^{\text{BR}}$ and $\pi_{\mathcal{V}_n}$ lie in tensor product of spaces and we only need to show the equation holds for 1-d functions. We prove the equation by induction. when $n = 1$, then according to [Theorem 1](#):

$$\begin{aligned} \hat{f}_1^{\text{BR}}(x) &= \begin{cases} 2f(\frac{1}{2})x & \text{if } x \leq \frac{1}{2} \\ 2f(\frac{1}{2})(1-x) + f(1)(2x-1) & \text{if } x > \frac{1}{2} \end{cases} \\ &= [-\frac{1}{2}f(0) + f(\frac{1}{2}) - \frac{1}{2}f(1)]\phi_{1,1}(x) + [-f(0) + f(1)]\phi_{0,1}(x) \\ &= \pi_{\mathcal{V}_1}[f](x). \end{aligned}$$

Suppose the equation holds for $n = k$, and WLOG, suppose $x \in (x_{k, \beta_k}, x_{k, \beta_k+1})$ for some $x_{k, \beta_k}, x_{k, \beta_k+1} \in \mathbf{X}_n$ and β_k is odd. So we have:

$$\begin{aligned} \hat{f}_k^{\text{BR}}(x) &= f(x_{k, \beta_k})\phi_{k, \beta_k}(x) + f(x_{k, \beta_k+1})\phi_{k, \beta_k+1}(x) \\ &= \sum_{n \leq k} \sum_{\beta \in B_n} c_{n, \beta} \phi_{n, \beta}(x) = \pi_{\mathcal{V}_k}[f] \end{aligned}$$

with $x \in \text{supp}[\phi_{n,\beta_n}]$ and $\beta_n \in B_n$. When $n = k + 1$, we have:

$$\begin{aligned}\pi_{\mathcal{V}_{k+1}}[f] &= \sum_{n \leq k+1} \sum_{\beta \in B_n} c_{n,\beta} \phi_{n,\beta}(x) \\ &= f(x_{k,\beta_k}) \phi_{k,\beta_k}(x) + f(x_{k,\beta_{k+1}}) \phi_{k,\beta_{k+1}}(x) + c_{k+1,\beta_{k+1}} \phi_{k+1,\beta_{k+1}}(x).\end{aligned}$$

According to the following identities:

$$\begin{aligned}x_{k,\beta_k} &= x_{k+1,\beta_{k+1}-1} \\ x_{k,\beta_k} &= x_{k+1,\beta_{k+1}+1}\end{aligned}$$

and, WLOG, conditioned on the assumption $x \in (x_{k,\beta_k}, x_{k+1,\beta_{k+1}})$, we have

$$\begin{aligned}\phi_{k,\beta_k}(x) &= \frac{x_{k,\beta_{k+1}} - x}{2^{-k}} \\ \phi_{k,\beta_{k+1}}(x) &= \frac{x - x_{k,\beta_k}}{2^{-k}} \\ \phi_{k+1,\beta_{k+1}}(x) &= \frac{x - x_{k,\beta_k}}{2^{-k-1}}.\end{aligned}$$

Now we plug in equation (42) and the above identities, we can have the result:

$$\begin{aligned}\pi_{\mathcal{V}_{k+1}}[f] &= f(x_{k+1,\beta_{k+1}-1}) \phi_{k+1,\beta_{k+1}-1}(x) + f(x_{k+1,\beta_{k+1}}) \phi_{k+1,\beta_{k+1}}(x) \\ &= \hat{f}_{k+1}^{\text{BR}}(x).\end{aligned}$$

□

A.2. Proof of Theorem 3

Proof. WLOG, we assume that the mean function $\mu = 0$. Let $f \in \mathcal{H}_{mix}^{1,c}$, then the difference between the two interpolator \hat{f}_n^{BR} and \hat{f}_n^{BM} conditioned on \mathbf{X}_k^{SP} can be written as

$$\begin{aligned}\delta(\mathbf{x}) &:= |\hat{f}_n^{\text{BR}}(\mathbf{x}) - \hat{f}_n^{\text{BM}}(\mathbf{x})| \\ &= |[f(\mathbf{x}) - \hat{f}_n^{\text{BR}}(\mathbf{x})] - [f(\mathbf{x}) - \hat{f}_n^{\text{BM}}(\mathbf{x})]|.\end{aligned}$$

We first define the following hierarchical difference functions:

$$\begin{aligned}\Delta_{\alpha_j}^{\text{BR}}[f](x_j) &:= \{k^{\text{BR}}(x_j, \mathbf{X}_{\alpha_j}) [k^{\text{BR}}(\mathbf{X}_{\alpha_j}, \mathbf{X}_{\alpha_j})]^{-1} - \\ &\quad k^{\text{BR}}(x_j, \mathbf{X}_{\alpha_{j-1}}) [k^{\text{BR}}(\mathbf{X}_{\alpha_{j-1}}, \mathbf{X}_{\alpha_{j-1}})]^{-1}\} f(\mathbf{X}_{\alpha_j}) \\ \Delta_{\alpha_j}^{\text{BM}}[f](x_j) &:= \{k_{\omega_j}^{\text{BM}}(x_j, \mathbf{X}_{\alpha_j}) [k_{\omega_j}^{\text{BM}}(\mathbf{X}_{\alpha_j}, \mathbf{X}_{\alpha_j})]^{-1} - \\ &\quad k_{\omega_j}^{\text{BM}}(x_j, \mathbf{X}_{\alpha_{j-1}}) [k_{\omega_j}^{\text{BM}}(\mathbf{X}_{\alpha_{j-1}}, \mathbf{X}_{\alpha_{j-1}})]^{-1}\} f(\mathbf{X}_{\alpha_j}).\end{aligned}$$

According to equation (2) and (3) in [Barthelmann, Novak and Ritter \(2000\)](#), we have the following expansion of the error terms:

$$f(\mathbf{x}) - \hat{f}_n^{\text{BR}}(\mathbf{x}) = \sum_{|\alpha| \geq k+d} \bigotimes_{j=1}^d \Delta_{\alpha_j}^{\text{BR}}[f](x_j)$$

$$f(\mathbf{x}) - \hat{f}_n^{\text{BM}}(\mathbf{x}) = \sum_{|\alpha| \geq k+d} \bigotimes_{j=1}^d \Delta_{\alpha_j}^{\text{BM}}[f](x_j)$$

where

$$\sum_{|\alpha| \geq k+d} \bigotimes_{j=1}^d \Delta_{\alpha_j}^{\text{BR}}[f](x_j) = \sum_{|\alpha| \geq k+d} f_{\alpha}(\mathbf{x})$$

We now want to write the expansion of $f(\mathbf{x}) - \hat{f}_n^{\text{BM}}(\mathbf{x})$ in terms of $\{\Delta_{\alpha_j}^{\text{BR}}[f](x_j)\}$. According to Theorem 2 in [Ding and Zhang \(2018\)](#), for any 1-d function $f \in \mathcal{H}_{\text{mix}}^{1,c}$, we can write the BLUE of kernel $k_{\omega_j}^{\text{BM}}$ explicitly:

$$\begin{aligned} & k_{\omega_j}^{\text{BM}}(x_j, \mathbf{X}_{\alpha_j}) [k_{\omega_j}^{\text{BM}}(\mathbf{X}_{\alpha_j}, \mathbf{X}_{\alpha_j})]^{-1} f(\mathbf{X}_{\alpha_j}) \\ &= \frac{\sinh[\omega_j(x_{\alpha_j, \beta_j+1} - x_j)]}{\sinh[\omega_j 2^{-\alpha_j}]} f(x_{\alpha_j, \beta_j}) + \frac{\sinh[\omega_j(x_j - x_{\alpha_j, \beta_j})]}{\sinh[\omega_j 2^{-\alpha_j}]} f(x_{\alpha_j, \beta_j+1}) \\ &= \frac{x_{\alpha_j, \beta_j+1} - x_j}{2^{-\alpha_j}} f(x_{\alpha_j, \beta_j}) + \frac{x_j - x_{\alpha_j, \beta_j}}{2^{-\alpha_j}} f(x_{\alpha_j, \beta_j+1}) + \mathcal{O}(2^{-2\alpha_j}) \\ &= k^{\text{BR}}(x_j, \mathbf{X}_{\alpha_j}) [k^{\text{BR}}(\mathbf{X}_{\alpha_j}, \mathbf{X}_{\alpha_j})]^{-1} f(\mathbf{X}_{\alpha_j}) + \mathcal{O}(2^{-2\alpha_j}) \end{aligned}$$

where x_{α_j, β_j} and x_{α_j, β_j+1} are the points that satisfy $x_j \in [x_{\alpha_j, \beta_j}, x_{\alpha_j, \beta_j+1}]$, the second equality of the above equation is from Taylor expansion, and the last equality is from the proof of Theorem 1. So the following equality holds:

$$\begin{aligned} \bigotimes_{j=1}^d \Delta_{\alpha_j}^{\text{BM}}(x_j) &= \bigotimes_{j=1}^d \{\Delta_{\alpha_j}^{\text{BR}}[f](x_j) + \mathcal{O}(2^{-2\alpha_j})\} \\ &= \bigotimes_{j=1}^d \Delta_{\alpha_j}^{\text{BR}}[f](x_j) + \sum_{j=1}^d \mathcal{O}(2^{-\alpha_j}) \bigotimes_{j=1}^d \Delta_{\alpha_j}^{\text{BR}}[f](x_j) \end{aligned}$$

where the second equality is from the fact that $\Delta_{\alpha_j}^{\text{BR}}[f](x_j)$ is in an order no smaller than $\mathcal{O}(2^{-2\alpha_j})$. Therefore, we can have the final result:

$$\begin{aligned} f(\mathbf{x}) - \hat{f}_n^{\text{BM}}(\mathbf{x}) &= \sum_{|\alpha| \geq k+d} \bigotimes_{j=1}^d \Delta_{\alpha_j}^{\text{BM}}[f](x_j) \\ &= \sum_{|\alpha| \geq k+d} \left[1 + \sum_{j=1}^d \mathcal{O}(2^{-\alpha_j}) \right] f_{\alpha}(\mathbf{x}) \\ &= \mathcal{O} \left(\sum_{|\alpha| \geq k+d} f_{\alpha} \right). \end{aligned}$$

□

A.3. Proof of Lemma 3

Proof. Let \mathbf{i} and \mathbf{h} denote (i_1, i_2, \dots, i_d) and $(2^{-\alpha_1}, \dots, 2^{-\alpha_d})$ respectively, and let \mathbf{ih} denote $(i_1 2^{-\alpha_1}, \dots, i_d 2^{-\alpha_d})$. Let $f(\mathbf{x}_I; \mathbf{x})$ denote f with fixed $x_i, i \notin I$. According to equation (42), we write $c_{\alpha, \beta}$ as

$$\begin{aligned}
c_{\alpha, \beta} &= \left(\prod_{i=1}^d A_{\alpha_i, \beta_i} \right) f(\mathbf{X}) \\
&= \sum_{i_d=-1}^1 \cdots \sum_{i_1=-1}^1 \left(\frac{-1}{2} \right)^{\sum_{j=1}^d |i_j|} f(\mathbf{x}_{\alpha, \beta} + \mathbf{ih}) \\
&= \sum_{i_d=-1}^1 \cdots \sum_{i_2=-1}^1 \left(\frac{-1}{2} \right)^{\sum_{j=2}^d |i_j|} \left(-\frac{1}{2} \right) \cdot \\
&\quad \int_{\mathbf{x}_{\alpha_1, \beta_1}}^{\mathbf{x}_{\alpha_1, \beta_1} + h_1} \partial_{x_1} [f(s_1; \mathbf{x}_{\alpha, \beta}) - f(s_1 - h_1; \mathbf{x}_{\alpha, \beta})] ds_1 \\
&= \left(-\frac{1}{2} \right)^d \int_{\mathbf{x}_{\alpha_d, \beta_d}}^{\mathbf{x}_{\alpha_d, \beta_d} + h_d} \cdots \int_{\mathbf{x}_{\alpha_1, \beta_1}}^{\mathbf{x}_{\alpha_1, \beta_1} + h_1} D^{\mathbf{1}} \sum_{i_1, \dots, i_d=0}^1 (-1)^{\sum_{j=1}^d |i_j|} f(\mathbf{s} - \mathbf{ih}) d\mathbf{s}.
\end{aligned}$$

When $d = 1$, any function in $\mathcal{H}_{mix}^{1,c} \subset \mathcal{H}^1(\mathcal{X})$ can be extended to trace-zero function, which is the limit of a sequence of smooth functions under the $\mathcal{H}_{mix}^{1,c}$ norm (Theorem 5.5.2 of Evans (2015)). When $d > 1$, any $f \in \mathcal{H}_{mix}^{1,c}$ is also the limit of a sequence of smooth functions $\{g^n\}$ under the $\mathcal{H}_{mix}^{1,c}$ norm because $\mathcal{H}_{mix}^{1,c}$ is the tensor product of 1-d function spaces. Therefore, according to Lebesgue differentiation theorem, for almost all $\mathbf{x} \in \mathcal{X}$:

$$\begin{aligned}
&\int_{\mathbf{x}}^{\mathbf{x}+h} |D^{\mathbf{1}} f(\mathbf{s}) - D^{\mathbf{1}} f(\mathbf{s} - h)| d\mathbf{s} \\
&\leq \int_{\mathbf{x}-h}^{\mathbf{x}+h} |D^{\mathbf{1}} f(\mathbf{s}) - D^{\mathbf{1}} g^n(\mathbf{s})| d\mathbf{s} + \int_{\mathbf{x}}^{\mathbf{x}+h} |D^{\mathbf{1}} g^n(\mathbf{s}) - D^{\mathbf{1}} g^n(\mathbf{s} - h)| d\mathbf{s} \\
&\leq Ch^{1+\gamma}
\end{aligned}$$

where the last line is because the first term of the second line can be arbitrarily small by letting n large from the trace-zero theorem and the second term is the difference of two smooth functions and hence we can use Hölder's condition to have an upper bound.

Now, WLOG, we assume $\alpha_1 = |\alpha|_{\infty}$ and then, as long as there is no singular

point \mathbf{x} that does not satisfy the Hölder condition near $\mathbf{x}_{\alpha,\beta}$, we can have:

$$\begin{aligned}
|c_{\alpha,\beta}| &= \left(\frac{1}{2}\right)^d \left| \int_{\mathbf{x}_{\alpha_d,\beta_d}}^{\mathbf{x}_{\alpha_d,\beta_d}+h_d} \cdots \int_{\mathbf{x}_{\alpha_1,\beta_1}}^{\mathbf{x}_{\alpha_1,\beta_1}+h_1} D^{\mathbf{1}} \sum_{i_1,\dots,i_d=0}^1 (-1)^{\sum_{j=1}^d |i_j|} f(\mathbf{s} - ih) d\mathbf{s} \right| \\
&\leq \left(\frac{1}{2}\right)^d \int_{\mathbf{x}_{\alpha_d,\beta_d}}^{\mathbf{x}_{\alpha_d,\beta_d}+h_d} \cdots \int_{\mathbf{x}_{\alpha_1,\beta_1}}^{\mathbf{x}_{\alpha_1,\beta_1}+h_1} \\
&\quad \sum_{i_2,\dots,i_d=0}^1 |D^{\mathbf{1}} f(s_1; \mathbf{s} - ih) - D^{\mathbf{1}} f(s_1 - h_1; \mathbf{s} - ih)| ds \\
&\leq Ch_1^\gamma \prod_{i=1}^d h_i \\
&= C2^{-\{\gamma|\alpha|_\infty + |\alpha|\}},
\end{aligned}$$

where the third line is from the inequality from Lebesgue differentiation theorem we proved previously. If the Hölder condition fails at a specific point, then we can begin with the second line of the above equation to derive that $|c_{\alpha,\beta}| = \mathcal{O}(2^{-|\alpha|})$ via the inequality:

$$\begin{aligned}
&\left(\frac{1}{2}\right)^d \int_{\mathbf{x}_{\alpha_d,\beta_d}}^{\mathbf{x}_{\alpha_d,\beta_d}+h_d} \cdots \int_{\mathbf{x}_{\alpha_1,\beta_1}}^{\mathbf{x}_{\alpha_1,\beta_1}+h_1} \\
&\quad \sum_{i_2,\dots,i_d=0}^1 |D^{\mathbf{1}} f(s_1; \mathbf{s} - ih) - D^{\mathbf{1}} f(s_1 - h_1; \mathbf{s} - ih)| ds \\
&\leq \frac{1}{2^d} 2^{-|\alpha|} \sum_{i_2,\dots,i_d=0}^1 \|D^{\mathbf{1}} f(s_1; \mathbf{s} - ih) - D^{\mathbf{1}} f(s_1 - h_1; \mathbf{s} - ih)\|_{L^2(\mathcal{X})}.
\end{aligned}$$

This proves the claim. □

A.4. Proof of Lemma 4

Proof. The result follows from direct calculations:

$$\begin{aligned}
& \sum_{i=0}^{\infty} x^i \binom{i+k+d-1}{d-1} \\
&= \frac{x^{-k}}{(d-1)!} \left(\sum_{i \geq 0} x^{i+k+d-1} \right)^{(d-1)} \\
&= \frac{x^{-k}}{(d-1)!} \left(x^{k+d-1} \frac{1}{1-x} \right)^{(d-1)} \\
&= \frac{x^{-k}}{(d-1)!} \sum_{j=0}^{d-1} \binom{d-1}{j} (x^{k+d-1})^{(j)} \left(\frac{1}{1-x} \right)^{(d-1-j)} \\
&= \sum_{j=0}^{d-1} \binom{d-1}{j} \frac{(k+d-1)!}{(k+d-1-j)!} x^{d-1-j} \frac{(d-1-j)!}{(d-1)!} \left(\frac{1}{1-x} \right)^{d-1-j+1} \\
&= \sum_{j=0}^{d-1} \binom{k+d-1}{j} \left(\frac{x}{1-x} \right)^{d-1-j} \frac{1}{1-x}.
\end{aligned}$$

□

A.5. L^P Convergence Rate without Boundary Information

Theorem 7. Let $f \in \mathcal{H}_{mix}^1$ and Φ be the kernel whose native space is equivalent to \mathcal{H}_{mix}^1 . Let \hat{f}_k^{SP} be the posterior mean of the GP with kernel Φ conditioned on a sparse grid design \mathbf{X}_k^{SP} with n design points. Then:

$$\|f - f_k^s\|_{L^\infty} = \mathcal{O}(n^{-\frac{1}{2}} [\log n]^{\frac{5}{2}(d-1)}).$$

Proof. We replace $|f(x+\delta) - f(x)|$ with $[\int_0^1 |f(x+\delta) - f(x)|^p dx]^{\frac{1}{p}}$ in equation (20) in [Rieger and Wendland \(2017\)](#) and use Hölder's inequality to get:

$$\int_0^1 |f(x+\delta) - f(x)|^p dx = \int_0^1 \left| \int_x^{x+\delta} f'(s) ds \right|^p dx \leq \delta^{\frac{1}{2}} \|f'\|_{L^2}.$$

As a result, we can have the following inequality:

$$\mathcal{E}(f; \pi_m(I))_{L^p} \leq cm^{-1+\frac{1}{2}} \|f\|_{\mathcal{H}^1}$$

where $\mathcal{E}(f; V)_{L^p}$ is the best approximation error for a given f from V measured in L^p norm and π_m is the set of polynomials of degree less than m . On the other hand, Theorem 8 in [Barthelmann, Novak and Ritter \(2000\)](#) also holds

true for \widehat{L}^p norm, therefore, by following the proof for Theorem 9 in [Rieger and Wendland \(2017\)](#), we can have the following inequality:

$$\|f\|_{L^p(T^d)} \leq C \binom{q-1}{d-1} n^{-\frac{1}{2}} [\log n]^{\frac{3}{2}(d-1)} \|f\|_{\mathcal{H}_{mix}^1} + \binom{q-d}{d-1} \max |f(\mathbf{X}_q^s)|.$$

We then replace f with $f - f_k^s$. Because f_k^s is exact on \mathbf{X}_q^{SP} the second term on the right hand side vanishes. We have shown in Theorem 5 that $\binom{q-1}{d-1} = \mathcal{O}([\log n]^{d-1})$ which leads to the final result. \square

A.6. Probabilistic Convergence Rate without Boundary Information

Theorem 8. Suppose $I^{[0]} \cup I^{[1]} = \emptyset$, and assume the sparse grid design \mathbf{X}_k^{SP} with $n = |\mathbf{X}_k^{\text{SP}}|$. Let $Z(\cdot)$ be a GP with kernel $k \in \mathcal{H}_{mix}^1(\mathcal{X} \times \mathcal{X})$ with no boundary information, and \mathcal{I}_n^s be the GP interpolation operator satisfying $\mathcal{I}_n^{\text{BM}} f = \widehat{f}_n^s$, where \widehat{f}_n^s is the posterior mean. Then:

$$\mathbb{E} \left[\sup_{\mathbf{x} \in \mathcal{X}} |Z(\mathbf{x}) - \mathcal{I}_k^s Z(\mathbf{x})|^p \right]^{\frac{1}{p}} = \mathcal{O}(n^{-\frac{1}{2}} [\log n]^{\frac{5}{2}d-2}), \quad 1 \leq p < \infty,$$

and

$$\sup_{\mathbf{x} \in \mathcal{X}} |Z(\mathbf{x}) - \mathcal{I}_k^s Z(\mathbf{x})| = \mathcal{O}_{\mathbb{P}}(n^{-\frac{1}{2}} [\log n]^{\frac{5}{2}d-2}).$$

Proof. We can follow the proof for Theorem 6, with the only difference being that for any kernel $k(\mathbf{x}, \mathbf{y}) \in \mathcal{H}_{mix}^1(\mathbb{R}^d \times \mathbb{R}^d)$ without boundary information, the uniform bound of the induced natural distance becomes:

$$\sigma(\mathbf{x}, \mathbf{y}) = \mathcal{O}(n^{-\frac{1}{2}} [\log n]^{\frac{5}{2}(d-1)}).$$

The claim can then be shown by performing the same substitution as in the proof in Theorem 6. \square